Mestrado Integrado em Engenharia Química

Olive mill wastewater valorization through H_2/CH_4 production

Tese de Mestrado

de

Ana Inês Dias da Silva

Desenvolvida no âmbito da unidade curricular de Dissertação

realizado em

Italian National Agency for New Technologies, Energy and Sustainable Economic Development

Orientador na FEUP: **Prof. Miguel Madeira**

Orientador no ENEA: **Eng. Silvano Tosti**

Departamento de Engenharia Química

Outubro de 2015

Acknowledgments

This thesis not only symbolizes the end of my course but is an expression of hard work and personal growth, not just in these 5 months but in the last 5 years. Years filled with both bad and good moments, bad and good decisions, which nevertheless, eventually took me here.

Firstly, I want to give a special thank you to my coordinators, Prof. Madeira (FEUP) and Eng. Silvano Tosti (ENEA), which without their patience, help and guidance this work would not be possible. Also I am grateful all the people who received me at ENEA. In special I give thanks to David, Alessia, Fabio and Mirko (for all their help and patience with me in the lab) and also Marco and Barbara. I further thank Vitória for her company throughout my staying in Rome, and all the people I met there.

Secondly, to my friends Anabela and Patricia for all their support over the years and for lessening the homesickness during my stay in Rome. It was hard, but without them it would be even unbearable. Also to my friends from FEUP which made these 5 years the best.

To my parents for all the support, patience and sacrifice to give me the opportunity to be part of this great experience. To my dear brother, who always grinds my years but without whom life would be boring. To all my family, and especially to my grandmother Elvira, who I wish would be here to see me.

Sumário

A *Olive Mill Wastewater* (OMW) é um material bastante problemático para a área Mediterrânica devido às suas grandes concentrações de fenóis e poluição orgânica, os quais contribuem para uma pobre degradabilidade e alta fitotoxicidade. Devido ao alto nível de compostos orgânicos, é possível gerar correntes ricas em hidrogénio, através de reações de *reforming*, e também produzir metano (por hidrogenólise). Consequentemente, OMW é convertida numa fonte de energia.

O objetivo deste trabalho é tratar OMW de forma a produzir hidrogénio por reações de *reforming* de vapor e reforming de vapor oxidativo usando um catalisador de 3 wt.% Pt / 10 wt.% Ni / CeO_2, e comparar os resultados com um trabalho anterior, onde se usou um catalisador diferente (Rh/Pt *washcoated*). É também estudada a produção de metano através da reação de *reforming* de etanol e OMW. Todos estes testes foram realizados num reator de membranas de Pd – Ag, com uma espessura de 150 μm, que tinha no seu interior com 12.08 de catalisador referido. Os testes para a produção de hidrogénio foram realizados a 450 ºC a uma pressão entre 1 e 5 bar. Os testes para a produção de metano foram realizados a 300 ºC e no mesmo intervalo de pressão.

A produção de hidrogénio por *reforming* de vapor foi muito reduzida, sendo que a maior quantidade de hidrogénio produzido foi de 10.67 sccm, aproximadamente 33% menor que o valor observado no trabalho anterior mencionado acima. A produção de hidrogénio nos testes de *reforming* de vapor oxidativo foi nula. Estes testes levaram à conclusão que o catalisador não é adequado para a produção de hidrogénio através destas reações, sendo que a razão provável para tal possa dever-se à desativação do catalisador e cinéticas reduzidas.

No caso da produção de metano, a maior produção observada foi de um rendimento de 33.3% para um teste realizado com etanol (10% v/v). Foi observada uma grande quantidade de produção de coque, que rapidamente desativa o catalisador.

Abstract

Olive mil wastewater (OMW) is a very problematic material in the Mediterranean regions due to its high levels of phenols and organic pollution, which contribute to a poor degradability and high phytotoxicity. Given its high amount of organic compounds, it is possible to generate hydrogen rich gas streams, through reforming reactions, and also produce methane (by hydrogenolysis). Consequently, OMW is converted in an energy source.

The aim of this work is to treat OMW to produce hydrogen through steam reforming (SR) and oxidative steam reforming (OSR) reactions using a 3 wt.% Pt / 10 wt.% Ni / CeO_2 catalyst, and compare the results with a previous work, which used a different catalyst (Rh/Pt washcoated). Also, it was studied the production of methane through hydrogenolysis reaction from both ethanol and OMW. All of this was performed in a 150 μm thick Pd - Ag membrane reactor filled with 12.08 g of the referred catalyst. The hydrogen production tests were performed at 450 ºC in the pressure range of 1 – 5 bar. The methane production tests were performed at 300 ºC and in the same pressure range.

The hydrogen production results from SR were very slim, being the highest hydrogen produced of 10.67 sccm, around 33% less than the production achieved in the previous work mentioned above. The production of hydrogen in the oxidative reforming tests was null. These tests lead to the conclusion that this catalyst is not adequate for the production of hydrogen through these reactions, the probable reason being the catalyst deactivation and low kinetics.

In the case of the methane production, the maximum achieved was with ethanol (10% v/v) which provided a yield of 63.3%. It was noted a high production of coke, which quickly deactivated the catalyst.

Declaração

I declare, under oath, that this work is original and that all non-original contributions were duly referenced with the reference of the source.

Contents

Figures Captions

Tables Captions

Notation and Glossary

List of Acronyms

ENEA	Italian National Agency for New Technologies, Energy and Sustainablem[2] Economic Development
SR	Steam Reforming
OSR	Oxidative Steam Reforming
WGS	Water-Gas Shift
MR	Membrane Reactor
GMFC	Gas Mass Flow Controller
FM	Flowmeter
LMFC	Liquid Mass Flow Controller
sccm	standard cubic centimeter per minute

Índexes

p	permeate
r	retentate

Nomenclature

A	Permeation surface area (m^2)
C	Hydrogen concentration ($mol.s^{-1}$)
D	Diffusion Coefficient ($m^2.s^{-1}$)
δ	Membrane thickness (m)
E_a	Activation energy for the permeation ($J.mol^{-1}$)
F_i	Feed Flow rate of species i (sccm)
P	Pressure (bar)
P_e	Hydrogen permeability ($mol.m^{-1}.s^{-1}.Pa^{-0.5}$)
$P_{e,0}$	Permeability pre-exponential factor ($mol.m^{-1}.s^{-1}.Pa^{-0.5}$)
S	Solubility coefficient ($mol.m^{-3}.Pa^{-0.5}$)
T	Temperature (K)

Constants

$R = 8.134\, J.mol^{-1}$

1. Introduction

Since its origin, Frascati's Research Center of ENEA (Italian National Agency for New Technologies and Sustainable Economic Development) has been focused in fusion technology, taking an active role in the European Fusion Program. Inserted in the fusion framework, the Membrane Laboratory develops and produces metallic membranes (Pd-Alloy) for the separation in gaseous phases of hydrogen and its isotopes. This laboratory's initial study concerned the production of Pd-Ag tubes which evolved to the development of different membrane module configurations (finger-like, use of metal bellows, multi-tube, etc.). Throughout the years, experiments on dehydrogenation processes (steam reforming, water gas shift, etc.) have been performed, primarily using hydrocarbons and alcohols and more recently evolving to the use of olive mill wastewater (OMW), a very polluting material which is a by-product of the olive oil industry.

Concerning the present work, an experimental set-up consisting of a Pd-Ag permeator tube attached to a membrane reactor in a "finger like" configuration was used. Initially, the membrane was characterized by being subjected to permeation tests at various temperatures and pressures, ranging from 300 ºC to 450 ºC and 1 to 5 bar, respectively. Following, a plan of action was made which consisted in reaction tests with a feed of different ratios of OMW/methane and two control tests of OMW/N_2 and H_2O/CH_4 were also planned. Due to bad results, the tests were not conclusive and an extra one was performed with the OMW from a previous work, by Presterà (2014), in order to: i) make sure some problems in the distillation did not affect the OMW and ii) to compare it with the hydrogen production obtained from said previous work. After these, a test of oxidative steam reforming with a feed of OMW/O_2 was also executed. Once again, as the hydrogen production was negligible, a different approach was adopted. Instead of targeting the production of hydrogen, OMW was used to form methane. This approach still addressed the polluting degree of the OMW, aiming reducing it, and at the same time producing carbon neutral methane.

1.1 Thesis Outline

This thesis is organized as follows:

Chapter 2 includes a state of the art of the olive mill wastewater and its possible involvement in an hydrogen economy, as well as the description of the reactions used in this work for the production of hydrogen and methane.

In Chapter 3 there is a description of the work performed throughout this thesis, the experimental set-up used and the experimental plan.

Chapter 4 contains the results obtained in every test performed and their discussion.

In Chapter 5 are resumed the experimental results as well as a reference for future work.

2. State of the Art

2.1 Olive Mill Wastewater

The olive oil industry is very important in Mediterranean countries, both in terms of wealth and tradition. Spain is the main world producer, alone being responsible for more than 50% of the European production, followed by Italy, Greece, and Portugal (International Olive Oil Council, 2014).

The extraction of olive oil generates huge amounts of wastes that may have a great impact on land, water and even on air environments, as reported by several studies. In particular, olive mill wastewater (OMW) has been the most pollutant and troublesome waste produced by olive mills, due to the following properties of this matter (Tsagaraki et al., 2007): strong offensive smell; extremely high degrees of organic pollution (chemical oxygen demand – COD – values up to 220 g L^{-1}) and a BOD_5/COD (BOD standing for biological oxygen demand) ratio between 0.2 (hardly degradable) and 0.4; pH between 3.0 and 5.9; high content of polyphenols (up to 80 g L^{-1}) which are not easily biodegradable and are toxic to most microorganisms; and high content of solid matter (total solids up to 20 g L^{-1}).

As a remark about its pollution impact, it is worth mentioning that 1 m^3 of OMW corresponds to 100-200 m^3 of domestic sewage (Tsagaraki et al., 2007). This waste, generated by both traditional and three-phase system mills, has been discarded accordingly to the countries laws or even illegally dumped, either way with high polluting consequences for the ecosystem. As an example, this impact can be comprised of natural water bodies contamination, decrease of soil fertility and damage of existing crops.

Due to the biotoxicity of its phenols content, OMW cannot be treated in a bioreactor, which is the common process of wastewater treatment plants, since it inhibits biological processes. Thus, the disposal of OMW is one of the main environmental problems affecting the Mediterranean area and recent research has been focusing on different treatment methods such as biological and thermal processes or methods for the production of fertilizers, biopolymers and biogas (Roig et al., 2006; Fiorentino et al., 2003; Tsagaraki et al., 2007).

One way to dispose of OMW is to take advantage of it being a biomass source, and therefore possible to recover energy from. In fact, when used for this purpose it is seen as a clean energy source: being a biomaterial, the CO_2 released from its combustion is considered to have been previously captured from the atmosphere during the plant's growth, hence it can be looked at as CO_2 neutral.

2.1.1 Olive Mill Wastewater and the Hydrogen Economy

It is well established that the oil age will eventually be replaced by the gas age, which is expected to be dominated by hydrogen, as seen in Figure 2.1. It has been seen a shift in the energy sources from solid to liquid fuels, around the industrial revolution in the 18th century, when the world energy demand met its need with the resort to fossil fuels namely oil. It is anticipated a transition from the later to gases, firstly natural gas and then hydrogen.

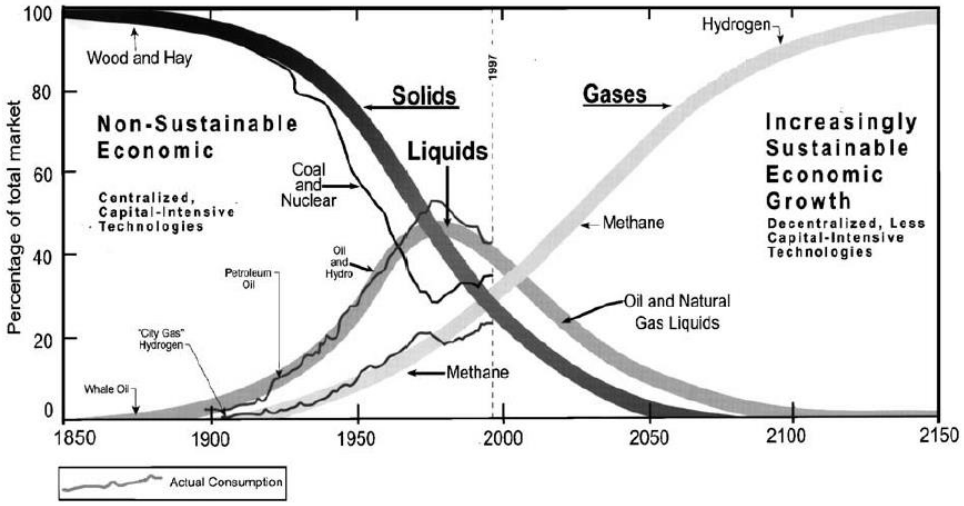

Figure 2.1 - Global energy systems transition (Dunn, 2002).

This belief is based on the fact that fossil fuels can no longer be considered sustainable. According to the International Energy Agency, IEA (2014), energy consumption is expected to increase 37% by 2040, referring to 2013. This is owing not only to the continued growth of the population, presently around 7 billion people, to over 9 billion by 2050, but also to the heavy industrialisation of developing continents, such as Asia and South America. Additionally, and according to Kjell et al. (2010), from now on the discovery of new oil fractions will not be able to compensate the decline in production of existing ones, which allows drawing the conclusion that the world has passed the peak of global oil production. If this is really the case, the world has reached the so called "Peak of the Oil Age" implying that oil will become increasingly more difficult to retrieve, thus more expensive.

Another contributing factor for the energy carrier shift from fossil fuels is related to environmental concerns around the CO_2–based greenhouse effect and air pollution, which in turn is known to be responsible for serious health problems. These issues, directly connected with carbon dioxide emissions, derived from the combustion of fossil fuels, motivate the need for a cleaner energy.

Considering all the previous statements, hydrogen seems to be the most suitable choice. Environmentally speaking it is considered a clean energy source, because its combustion

produces only water, and it is energetically advantageous, since the energy associated with the combustion process (~141.9 kJ g^{-1}) is about three times larger than that of traditional fuels (~47.5 kJ g^{-1}) (Dincer and Acar, 2015). Moreover, it is abundantly distributed throughout the world regardless of national boundaries.

With this in mind, the world would face a shift in the energy economy from fossil fuels to hydrogen. The hydrogen economy, illustrated in Figure 2.2, could be described as a network linking hydrogen's primary sources to its possible uses (Crabtree et al., 2004).

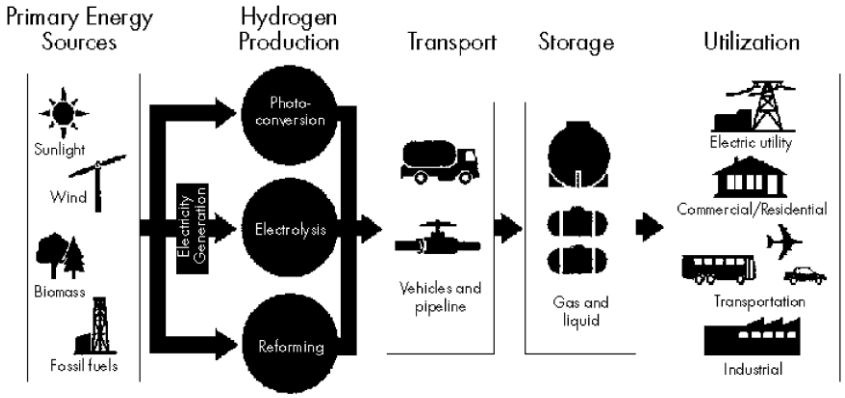

Figure 2.2 – The hydrogen economy (Dunn, 2002)

As hydrogen is not an energy source *per se* but an energy carrier, it connects all the sectors, linking the primary sources of energy to its possible applicabilities (as seen in Figure 2.2). It can be produced not only from the main feedstocks reported above (fossil fuels or water), but also using renewable sources such as solar, wind, biomass or nuclear.

In fact, with respect to renewable energies, hydrogen can be a solution when energy production exceeds the energy consumption, causing the energy grid to overload. Taking as example the wind power production in Denmark, although in average it only accounts for less than 20% of the energy consumption (Jørgensen and Ropenus, 2008), there are periods when an excess of wind power is produced that the power grid is too weak to accommodate. Instead of reinforcing the grid to be able to store the excess of energy, a hypothesis was studied where the excess of energy would be stored as hydrogen, a process commonly known as *Power to Gas* (*PtG*). This study found that the price for producing hydrogen through this method is very high when compared to the milestone the Department of Energy of the United States, DOE, set to 2015 (16 €/GJ against 32–35 €/GJ). Nevertheless, there might be a change of scenario in the future. Owing to efficiency improvements and increasing fossil fuel prices, integrated systems might become economically competitive (Jørgensen and Ropenus, 2008).

Another aspect which corroborates this change in fuel economy is a report by Morris and Pehnt (2014), initiative of the Heinrich Böll Foundation. There it is stated that Germany assumes a

responsibility towards a greener energy efficiency by making a continuous energy transition from coal and nuclear energy to renewables, with biomass, wind and solar energies in the lead, by 2050. As Denmark, they also take hydrogen as a solution for wind and solar exceeded energy production in order to not overload the power grid. Currently there is a project to implement hydrogen in the transportation sector, already in the last phase, culminating in 2016 with a market preparation. Already there are public transports in some cities using fuel cells. According to this project, until the end of 2015 are planned 50 hydrogen refuelling stations scattered through Germany, in order to expand the fuel cells network to private cars (NOW, 2014).

The process *PtG* is the production of a high-energy density gas via electrolysis of water. Thus, the primary product of this process is hydrogen, which can later be converted to synthetic methane. The idea of storing energy in the form of methane was also proposed by the Energy research Centre of the Netherlands (ECN). Although this process requires multi-steps (electrolysis to hydrogen and methanation for the production of CH_4), which may reduce its efficiency, it would also be taking advantage of the existing infrastructure (to where methane, contrary to hydrogen, can be fed without many limitations) and the utilization of CO_2 (either from fermentation of biogas, gasification of bio-syngas or CO_2 capture) (Sarić et al., 2014).

Feedstocks can be processed through various technologies to produce hydrogen, such as water electrolysis, biomass reforming, PV electrolysis, *etc*. All of the production processes from a renewable feedstock are under development, either to increase hydrogen purity or in order to increase the hydrogen production itself.

During the course of this work, an approach towards the handling of OMW was studied, with the goal of introducing this material, as a biomass, in a hydrogen-based economy. As such, a way of producing hydrogen, by the steam reforming reaction (SR) and oxidative steam reforming reaction (OSR), was studied. Moreover, and as detailed later on, the possibility of using such waste for producing methane was studied as well.

When OMW is used to produce hydrogen (or methane), it constitutes a sustainable and ecological approach since at the same time the polluting side of this wastewater is also being addressed. Particularly relating to this work, OMW's high phenols content makes it feasible to produce hydrogen through reforming reactions in a metal-based membrane reactor. The main idea behind is to use hydrogen perm-selective membranes to shift to the products side the reforming reversible reactions, while simultaneously producing a pure / ultra-pure hydrogen stream (in the permeate side).

2.2 Membranes Technology

As referred previously, a membrane reactor can be used for the production of pure hydrogen from OMW, using a noble metal based catalyst.

According to IUPAC (Koros et al., 1996), a membrane reactor (MR) is a device for simultaneously performing a reaction and a membrane-based separation in the same physical device. This selective extraction permits obtaining higher hydrogen yields since the reaction conversion shifts towards the products, as stated by the Le Chatelier's principle.

2.2.1 Palladium – Silver Membranes

A wide range of membrane types can be used with MRs, from dense metallic to porous ceramic ones, the choice resting on the device's goal. Particularly for hydrogen production, metallic membranes have been studied mainly due to their capacity to prevent the permeation of larger molecules (such as CO, CO_2, O_2, N_2, etc.) through their dense metal wall, translating in a high selectivity towards hydrogen. Of said membranes, palladium-based ones are favoured for their high permeability and selectivity to hydrogen and high catalytic surface, which rapidly dissociates hydrogen molecules to form atomic hydrogen that permeates the lattice, as detailed in the next section. There are metals with higher values of permeability than palladium (such as Nb, Ta and V), which are characterised by high values of solubility and are therefore more prone to degradation through embrittlement, being consequently less durable (Ockwig and Nenoff, 2007).

Palladium is a very costly metal. In reality, its cost is around 4 times higher than that of gold. This led to the study of methods to reduce the amount of palladium in membranes while still keeping high selectivity and permeability values. These methods comprised the addiction of an alloy material and the reduction of the membrane thickness (Morreale, 2002).

A property of palladium that needs to be taken into account when choosing an alloy has to do with its behaviour in the presence of hydrogen. When hydrogen is fed through a membrane, it interacts with the metal lattice by being uploaded, therefore expanding it. Consequently, several surface effects (such as cracks or pinholes) may occur due to loss of ductility, as well as reduction of selectivity towards hydrogen. This problem, commonly referred to as embrittlement, usually takes place at low temperatures (< 300 ºC) and can be minimized by alloying Pd with Ag, Cu or Au. Silver is the alloy material with which higher permeabilities are achieved as well as improved mechanical properties while reducing the membrane cost (Gallucci et al., 2011).

In accordance, Pd-Ag membranes, with thin metal walls, have been studied and are now commercially available, usually with a content of 25 wt.% of silver (Morreale, 2002).

2.2.2 Hydrogen Permeation Through a Dense Metallic Membrane

The hydrogen permeation through a dense metal membrane occurs according to the Sievert's law. This states that, the hydrogen flux is proportional to the difference of the square root of the hydrogen partial pressures (in the permeate and retentate side) and inversely proportional to the membrane thickness. It takes place in 5 steps (Tosti, 2010):

1. Adsorption of the hydrogen molecule on the metallic surface.
2. Dissociation of the hydrogen molecule into atoms (metallic surface).
3. Diffusion of the dissociated hydrogen through the membrane.
4. Recombination of the hydrogen atoms in the permeate side of the membrane.
5. Desorption of the hydrogen molecule.

The mechanism described, also referred to as hydrogen permeation, is illustrated in Figure 2.3.

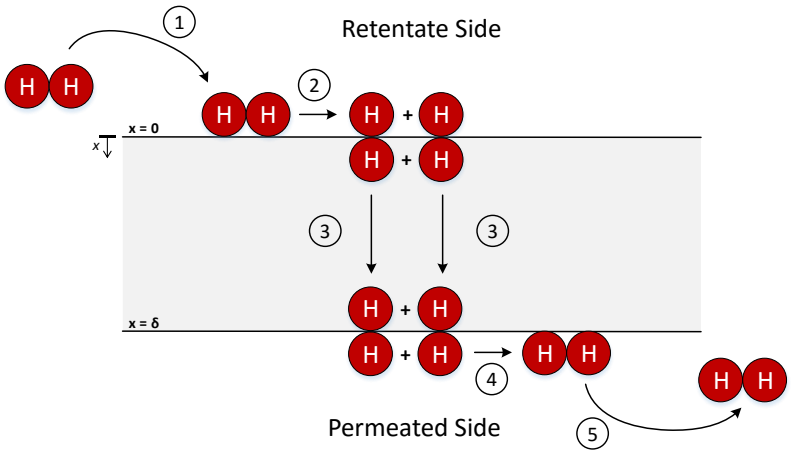

Figure 2.3 – Scheme of the transport mechanism of hydrogen through dense membrane materials (Adapted from Morreale (2002))

In this case, the steps of adsorption/desorption and diffusion through the membrane lattice control the permeation rate.

The diffusion of the hydrogen atoms through the membrane takes place according to Fick's law:

$$J = -D\frac{\partial C}{\partial x} \tag{2.1}$$

where *J* is the hydrogen flux being permeated through the membrane (mol m^{-2} s^{-1}), *D* is the diffusion coefficient (m^2 s^{-1}), C is the hydrogen concentration (mol m^{-3}) and x the position in the membrane (m).

The amount of hydrogen permeated through a membrane per unit area, at steady state and considering a constant diffusion coefficient, is given by the integration of equation (2.1) between both sides of the membrane:

$$J = -D\frac{C_p - C_r}{\delta} \tag{2.2}$$

being δ the membrane thickness and the indexes *p* and *r* the permeate and retentate sides, respectively.

In a quasi-equilibrium state, the hydrogen concentration into the metal is proportional to a solubility coefficient, *S* (mol m^{-3} $Pa^{-0.5}$), and to the square root of the hydrogen partial pressure in the gas phase, P_{H_2} (Pa):

$$C = S{P_{H_2}}^{0.5} \tag{2.3}$$

By combining equations (2.2) and (2.3), we obtain the equation which describes the hydrogen flux being permeated through the membrane:

$$J = P_e\frac{{P_{H_2,r}}^{0.5} - {P_{H_2,p}}^{0.5}}{\delta} \tag{2.4}$$

where $P_{H_2,r}$ and $P_{H_2,p}$ are the hydrogen partial pressures on the retentate and permeate side, respectively, and P_e, the permeability coefficient (mol m^{-1} s^{-1} $Pa^{-0.5}$), is given by:

$$P_e = SD \tag{2.5}$$

The permeability coefficient, being a function of temperature, can be described as an Arrhenius-type relation:

$$P_e = P_{e,0}e^{\left(\frac{-E_a}{R.T}\right)} \tag{2.6}$$

being $P_{e,0}$ (mol m^{-1} s^{-1} $Pa^{-0.5}$) the pre-exponential permeability coefficient, E_a (J mol^{-1}) the activation energy, *R* the gas constant (8.314 J mol^{-1} K^{-1}) and *T* the absolute temperature (K).

The pressure exponent, *n*, from equation (2.3), related to the Sievert's law, can take up several values, in a range from 0.5 to 1, as estimated by several studies. The hydrogen flux, *J*, depends on the membrane thickness, as can be seen in equation (2.4). In this case, the exponent *n* is equal to 0.5, obeying to the Sievert's law, and the rate limiting step is the bulk diffusion. However, if the permeation was limited by another transport phenomenon, the dependence on

the membrane thickness would consequently change, thus increasing the value of *n* (Li et al., 2008).

2.3 Hydrogen Production

For the production of H_2, hydrocarbons or alcohols, for example, react with water (steam), with or without the presence of O_2, in order to produce carbon monoxide and hydrogen (this mixture being so called syngas). This is followed by the water gas shift (WGS) reaction, where the carbon monoxide reacts with water and is converted into carbon dioxide and hydrogen, increasing the production and purity of the later.

2.3.1 Steam Reforming of Hydrocarbons

As mentioned above, there are two major reactions involved in the production of H_2 in a membrane reactor: steam reforming (SR) and WGS.

The steam reforming reaction of a generic hydrocarbon is:

$$C_nH_m + nH_2O \leftrightarrow nCO + (n + m/2)H_2 \quad (2.7)$$

For methane (*n*=1), presently the most used hydrocarbon raw material, the equation becomes:

$$CH_4 + H_2O \leftrightarrow CO + 3H_2 \qquad \Delta H^0_{298} = +206\ kJ\ mol^{-1} \quad (2.8)$$

To the steam reforming reaction typically follows the WGS reaction:

$$\mathrm{CO} + H_2O \leftrightarrow H_2 + CO_2 \qquad \Delta H^0_{298} = -41\ kJ\ mol^{-1} \quad (2.9)$$

The overall reaction for methane is given by equation (2.10).

$$CH_4 + 2H_2O \leftrightarrow CO_2 + 4H_2 \qquad \Delta H^0_{298} = +165\ kJ\ mol^{-1} \quad (2.10)$$

As the methane steam reforming reaction is highly endothermic and implies an increase in the number of moles from the reactants to the products side, from the thermodynamic point of view it is favoured by high temperatures and low pressures.

However, there may also occur some side reactions:

- the *Sabatier* reaction

$$CO_2 + 4H_2 \leftrightarrow CH_4 + 2H_2O \qquad \Delta H^0_{298} = +247\ kJ\ mol^{-1} \quad (2.11)$$

- the *Boudouard* reaction

$$2CO \leftrightarrow CO_2 + C \qquad \Delta H^0_{298} = -173\ kJ\ mol^{-1} \quad (2.12)$$

- the methanation reaction of CO

$$CO + 3H_2 \leftrightarrow CH_4 + H_2O \qquad \Delta H_{298}^0 = -206\ kJ\ mol^{-1} \tag{2.13}$$

- hydrocarbon cracking reactions (in this case, for methane)

$$CH_4 \leftrightarrow \mathrm{C\ (s)} + 2H_2 \qquad \Delta H_{298}^0 = +74\ kJ\ mol^{-1} \tag{2.14}$$

Both the Boudouard and the cracking reactions could be responsible for the deactivation of the catalyst, through coke deposition.

2.3.2 **Steam Reforming of Olive Mill Wastewater**

The high hydrogen content of alcohols, along with their easy accessibility, safeness in storage, management and non-toxicity, make them good candidates for hydrogen production. In fact, as referred before, bio-ethanol, produced from biomass, is being studied for that purpose since it is a way of valuing and disposing of that material. Another main advantage is that the CO_2 produced is considered neutral.

The steam reforming reaction, for a generic alcohol is as follows:

$$C_nH_{2n+1}OH + (n-1)H_2O \rightarrow nCO + 2nH_2 \qquad \Delta\mathrm{H} > 0 \tag{2.15}$$

For OMW, the reaction of a generic alcohol (1.15), coupled with the WGS reaction, can be considered to discuss the results of the thermodynamic tests (Tosti et al., 2015):

$$C_nH_{2n+1}OH + (2n-1)H_2O \rightarrow nCO_2 + 3nH_2 \qquad \Delta\mathrm{H} > 0 \tag{2.16}$$

There are also some side reactions to this process such as the steam reforming leading to CO and H_2 (2.15), the *Boudouard* reaction (eq. (2.12)) and the following ones, for the particular case of ethanol (Palma et al., 2012):

- Hydrogenolysis to methane

$$C_2H_5OH + 2H_2 \rightarrow 2CH_4 + H_2O \qquad \Delta H_{298}^0 = -157\ kJ\ mol^{-1} \tag{2.17}$$

- Cracking to methane and CO_2

$$C_2H_5OH \rightarrow 0.5CO_2 + 1.5CH_4 \qquad \Delta H_{298}^0 = -74\ kJ\ mol^{-1} \tag{2.18}$$

- Cracking to methane, CO, and H_2

$$C_2H_5OH \rightarrow CO + CH_4 + H_2 \qquad \Delta H_{298}^0 = +49\ kJ\ mol^{-1} \tag{2.19}$$

- Cracking to carbon, methane and water

$$C_2H_5OH \rightarrow CH_4 + C + H_2O \qquad \Delta H_{298}^0 = -82\ kJ\ mol^{-1} \tag{2.20}$$

As in the previous example, the *Boudouard* and the cracking reaction could be the responsible ones for the deposition of coke, and consequent deactivation of the catalyst.

2.3.3 Oxidative Steam Reforming

Many studies suggest that there is another process to produce hydrogen from bio-ethanol, more effective and energy efficient compared with conventional steam reforming reactions. This process combines the steam reforming reaction and the partial oxidation reaction and is named oxidative steam reforming reaction (OSR). Essentially the idea behind it is that the heat required by the endothermic steam reforming is provided by the oxidation of the alcohol.

The overall OSR reaction is described by the following equation.(de Lima et al., 2008)

$$C_2H_5OH + 2H_2O + 0.5O_2 \rightarrow 2CO_2 + 5H_2 \qquad \Delta H = -50\ kJ\ mol^{-1} \tag{2.21}$$

Being an exothermic reaction, from the thermodynamic point of view it is favoured at lower temperature. The side reactions that might arise are the same as the SR process ones, in addition to the ones that occur when oxygen is present (Vaidya and Rodrigues, 2006):

$$CO + {}^1/_2\, O_2 \rightarrow CO_2 \tag{2.22}$$

$$C_2H_5OH + {}^1/_2\, O_2 \rightarrow CH_3CHO + H_2O \tag{2.23}$$

$$CH_4 + 2O_2 \rightarrow CO_2 + 2H_2O \tag{2.24}$$

$$C + O_2 \rightarrow CO_2 \tag{2.25}$$

2.4 Methane Production

Methane can be produced from OMW through the hydrogenolysis reaction:

$$C_2H_5OH + 2H_2 \rightarrow 2CH_4 + H_2O \qquad \Delta H^0_{298} = -157\ kJ\ mol^{-1} \tag{2.17}$$

This reaction is favoured, from the thermodynamic point of view, at low temperatures. The side reactions include the reactions (2.17) to (2.20) as well as the *Sabatier* reaction (2.11) and the *Boudouard reaction* (2.12), referred above as side reactions to the steam reforming.

Instead of an electrolysis process, which consumes a lot of energy, with this process it is possible to attend to the fact that the existing infrastructures are not prepared for hydrogen storage, converting it into methane; moreover it also decreases the polluting degree of the OMW.

3. Technical Description

3.1 Pre-Treatment of the Olive Mill Wastewater

The olive mill wastewater (OMW) used in this work was obtained from an olive mill at Frascati (Italy) named *Ubertini*, in October, 21st of 2013. It was preserved at -20 ºC, which should be enough to stop any biological process such as fermentation or degradation. It consisted of a dark brown liquid with a very pungent and repulsive smell, where a white matter had formed on top (Fig. 3.1). This white matter is probably originated by the presence of fungus.

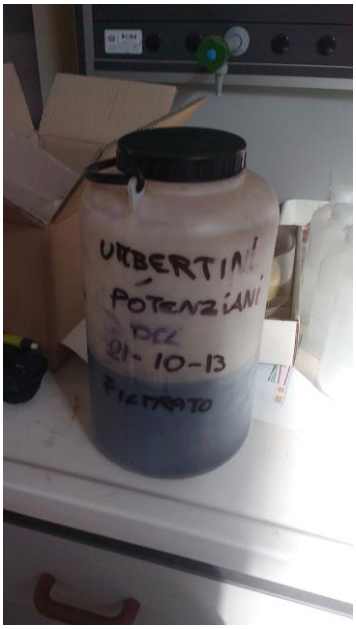

Figure 3.1 - Olive mil wastewater, from the "Ubertini" mill.

The OMW had to undergo a filtration, in order to remove any solid deposit, followed by a distillation, with the purpose of removing 50% of the water content, before being used in the membrane reactor. The removal of the solid deposit is also translated in the removal of organic load.

3.1.1 Filtration

The OMW filtration was performed using two filters (Figure 3.2). The first one was a primary coarse filtration, done with a square mesh of 0.97 mm x 0.97 mm, from which it was obtained

the white matter and some larger solid particles. The second filtration was made with a steel filter with a 0.12 mm x 0.12 mm mesh.

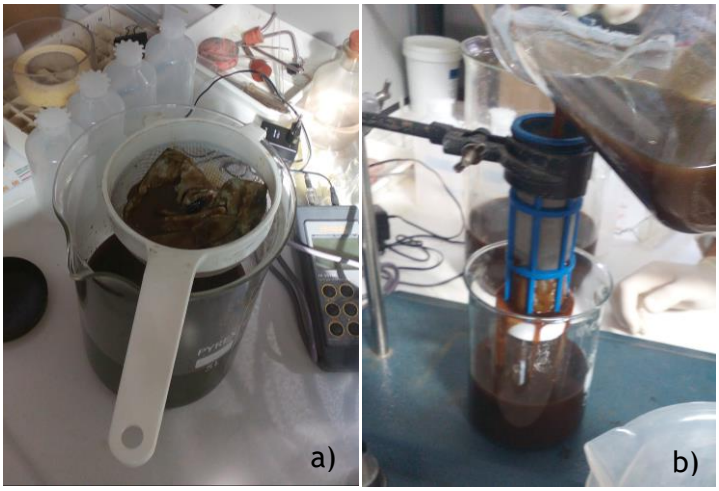

Figure 3.2 – Filters employed: a) square mesh; and b) steel mesh.

After the filtration, the pH and density of the resulting OMW were assessed. The pH was measured with a *pH-metro HANNA* meter, *"mod.HI 98150"*. The filtered OMW had a pH of 5.32 and a density of 1 g mL^{-1}.

3.1.2 Distillation of the Olive Mill Wastewater

Before being fed to the membrane reactor, the filtered wastewater was distilled in order to separate the fraction rich in water (about 50% v/v) and some residual solid, which remained from the filtration.

The equipment used consisted in a distillation balloon which was connected to a Graham condenser through a side-arm distilling head. The condensed fractions were collected in a Büchner flask. The balloon was wrapped in glass wool and tin foil and was heated by a resistance. The temperature of the mixture being distilled was measured by 2 thermocouples placed inside and above the liquid in order to obtain the liquid and vapour temperature, respectively. The distillation column was refrigerated with water at ambient temperature flowing in counter current, in order to obtain a more effective heat exchange. Figure 3.3 illustrates the set up described.

Figure 3.3 – Distillation apparatus.

During distillation are recovered three fractions (A, B and C), as described in Figure 3.4. Fraction B (about 65%) is supposedly constituted in its entirety by water while light and heavy compounds compose fractions A (about 20%) and C (about 15%), respectively. As such, several distillations of about 200 mL of OMW each were performed, of a total of approximately 2 L. Fraction A started distilling at approximately 86 ºC (for approximately 2 h), finishing at about 89 ºC, at which temperature fraction B started being collected (during approximately 4 h). At the temperature range of approximately 91 ºC fraction B finished distilling and fraction C was collected onwards (about 45 min).

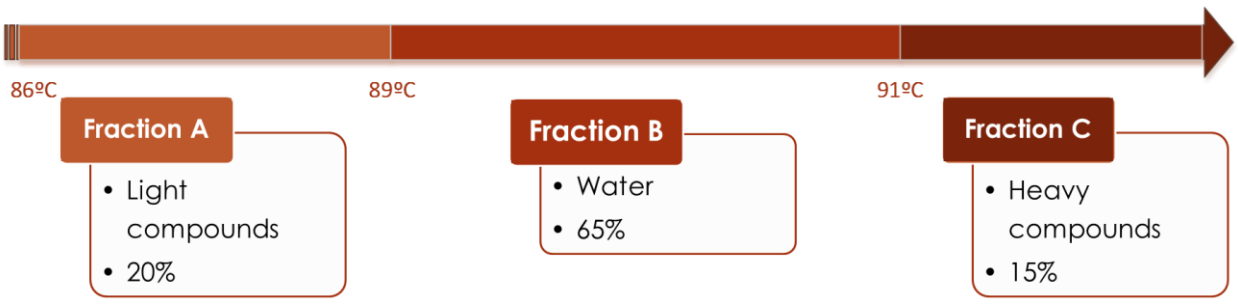

Figure 3.4 – Scheme of the distillation.

In total 2024 mL of filtered OMW were firstly distilled through ten distillations. At the end a comparison was performed between results achieved and the ones from a previous work, where

the same OMW was used. It was found that now the volume fraction of B was substantially higher than in the previous work. The differences between both works can be due to the replacement of the heating resistance and/or thermocouples. As such, it was decided to perform a distillation of the fraction B in order to retrieve the remainder volume of fractions A and C. In Table 3.1 is explicit a summary of the results obtained after both distillations and in the previous work by Gaetano (2014).

Table 3.1 - Summary of the distillation results

	V_{Total}	V_A		V_B		V_C		V_{A+B+C}/V_{Total}
	mL	mL	%	mL	%	mL	%	%
Present work	2024.0	410.8	20.3	1223.7	60.5	272.0	13.4	94.2
Presterà (2014)	3521	932	26.5	1967	55.9	396	11.3	93.6

Comparing the results with the ones from the previous work, it can be observed that some percentage of fraction A (approximately 5%) was not separated from fraction B. Apart from that discrepancy, both fraction C and the wasted matter (the solid fraction and some leaked material) are in line with the results from the previous work by Presterà (2014).

At the end of the distillation it was collected a fraction in its majority composed of water, which corresponded to 60% of the filtered OMW, and about 680 mL of fractions A and C, which will be fed to the membrane reactor.

3.1.3 Chemical Analysis of the Distilled Fractions

Both the mixture of fractions A and C as well as fraction B and the solid residue from the distillation were analysed in terms of phenols content. This analysis was performed by the Laboratory of Sanitary Engineering of the University of Naples Federico II according to APHA standard method 5550 B, using the Folin-Ciocalteau reagent (APHA et al., 2005). The calibration curve was established from the preparation of standards at increasing concentrations of phenol (C_6H_5OH), using pure phenol in crystals from Carlo Erba Reagenti. Folin-Ciocalteau reagent was purchased from Carlo Erba Reagenti. Sodium tartrate, sodium carbonate, and sodium sulphate anhydrous were acquired from Sigma Aldrich. Spectrophotometric measures were acquired by means of a Photolab 6600 UV-Vis spectrophotometer from WTW. In Table 3.2 are presented the data obtained along with results from previous works.

Table 3.2 – Chemical analysis results of the distilled fractions and solid residue.

Sample	pH	T (ºC)	Conductivity (µS)	Total phenols (mg L^{-1})	
Solid Residue				51886.0	
Fraction B	3.7	25	73	14.1	Present work
	4			30.3	Presterà (2014)
Fractions A+C	3.7	25	108	54.5	Present work
	4.0			123.7	Presterà (2014)
	3.2			23.8	Tosti et al. (2013)

As can be perceived, the total phenolic content is in general in line with the previous works. Although there is some disparity of the value for fractions A and C in the previous works, the present one's can be accepted as in the range of variability.

1.1 Experimental Set Up

The experimental set up used at ENEA during this work is illustrated in Figure 3.5

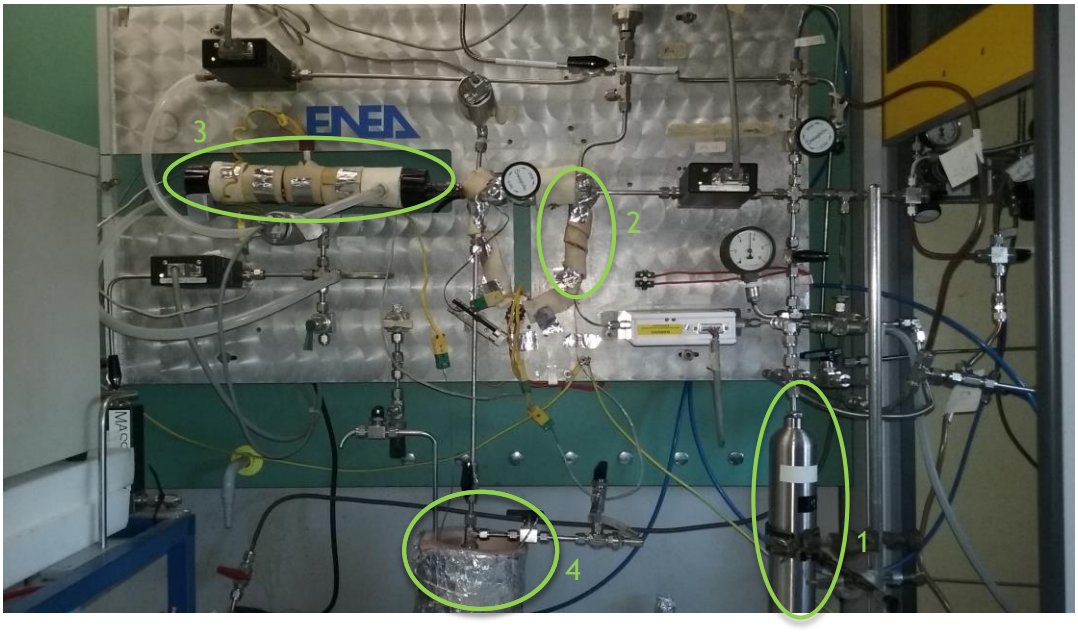

Figure 3.5 - Experimental set up where can be seen (1) the liquid tank, (2) the vaporizer, (3) the membrane reactor and (4) the condenser.

Figure 3.6 schematizes the experimental set up used in the permeation and reaction tests for the production of hydrogen, while Figure 3.7 depicts the one used in the reaction tests for the production of methane.

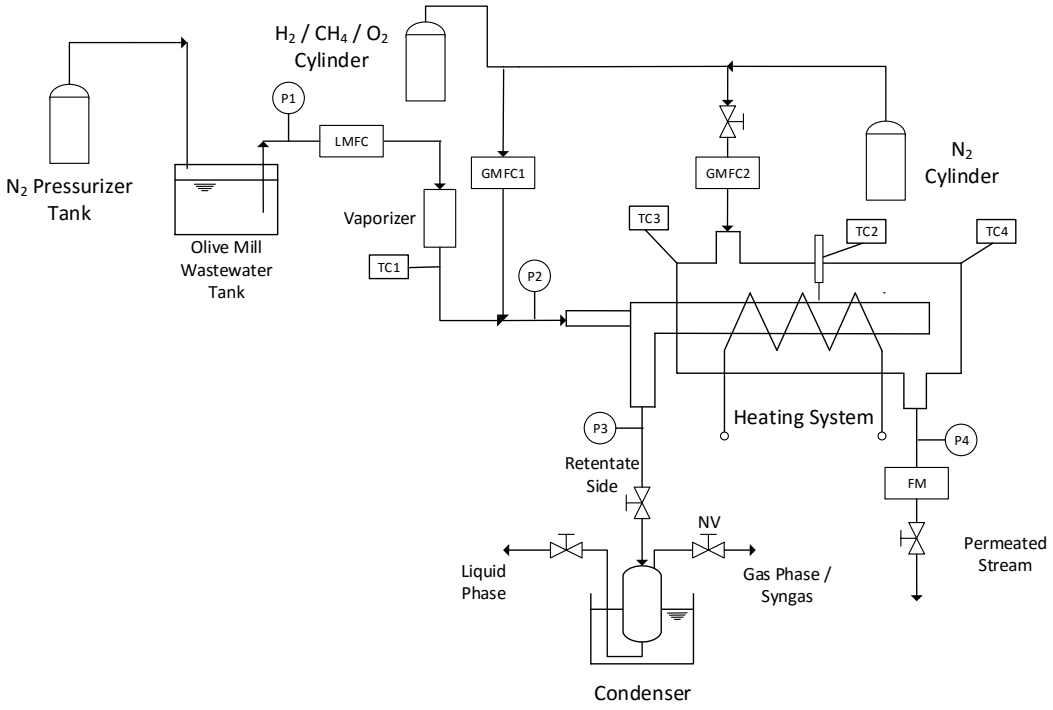

Figure 3.6 – Scheme of the experimental set up used in the permeation and reaction tests for the production of hydrogen.

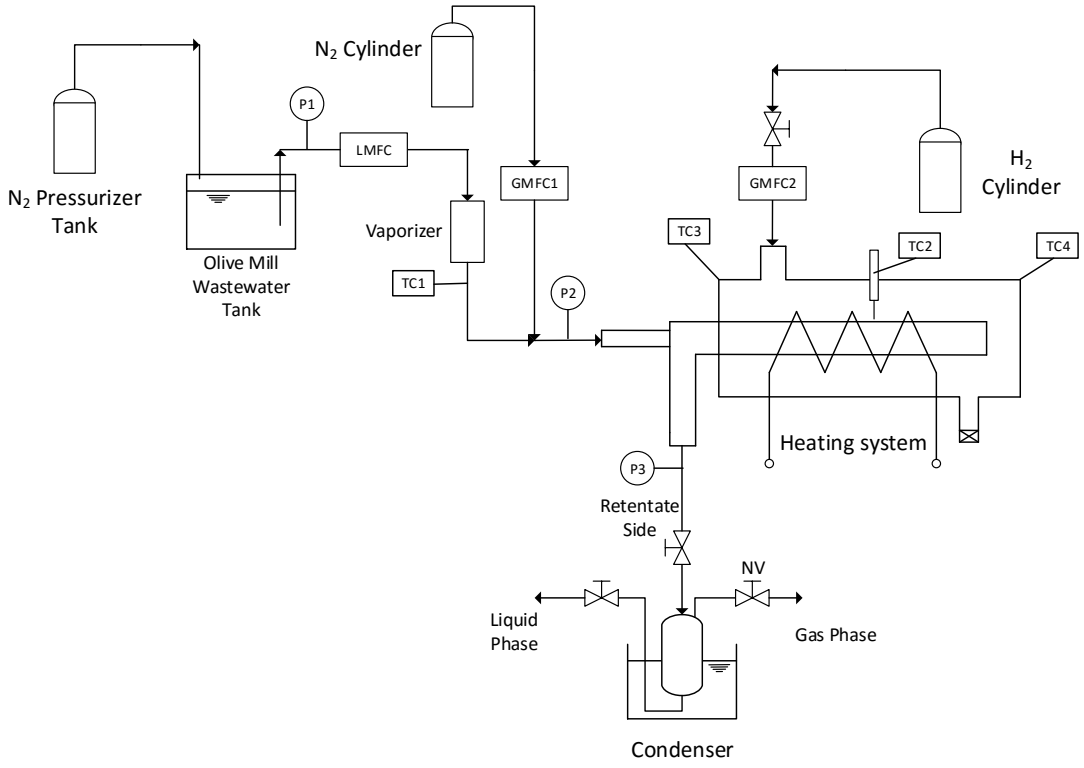

Figure 3.7 - Scheme of the experimental set up used in the reaction tests for the production of methane.

For the sake of organization, the following areas of the set-up were selected to be analysed in further detail:

- feed
- vaporization
- membrane reactor
    - methane production
- permeated side
- retentate side
- acquisition and control system
- chromatograph

3.1.4 **Feed**

In general there are three types of reagents used in this work: the liquid ones, the gases fed to the membrane and the gases fed to the shell.

The liquid reagents (water, OMW and ethanol) used in the reaction tests are fed from a liquid tank pressurized with nitrogen. The pressure is assured by a nitrogen tank and its value is measured through a barometer (P1) – cf.Fig. 3.6. The liquid fed to the membrane is quantified and controlled by a liquid meter flow controller (LMFC), from Brooks QUANTIM™, model QMAC500 (Maximum capacity: 50 g h^{-1}). Before being fed to the membrane, the liquid has to be vaporized, as detailed in the next section.

Concerning the gases fed to the membrane, methane and oxygen were stored in a gas bottle near the set up while nitrogen was fed from an external tank. In the case of hydrogen during the permeation tests and regeneration of the membrane (throughout the OS and OSR reactions) it was provided from an external tank, but just before the methane formation reactions it was substituted by a hydrogen generator, "Packard mod. 9400". The flow rate of gas was measured and controlled by the gas mass flow controller "MKS 1179B" (GMFC1 – cf. Fig. 3.6) (maximum capacity: 8.33×10^{-6} m^3 s^{-1} (500 sccm). The flow rates indicated refer to standard conditions (atmospheric pressure and 0 ºC of temperature). From now on all flow rates will refer to these conditions.

The gases fed to the membrane module shell are nitrogen and hydrogen. As the ones fed to the membrane feed, they come either from a liquid tank in the vicinity of the set up or placed in

the exterior. They are measured and controlled by a gas mass flow controller (GMFC2) "MKS 1179B" (maximum capacity: $16.66x10^{-6}$ m^3 s^{-1} (1000 sccm).

3.1.5 Vaporization

Before being fed to the membrane, the liquid stream has to be vaporized. This is achieved by means of a 90% Ni/10% Cr wire, functioning as a resistance, wrapped around the stainless steel tube. The resistance area is insulated and the temperature is measured with a K-type thermocouple (TC1), located right after said area – cf. Fig. 3.6.

3.1.6 Membrane Reactor

The membrane reactor consisted of a Pd-Ag permeator tube, which was brazed at its ends to two stainless steel tubes and filled with a catalyst, and then connected to a pyrex shell in a finger-like configuration – cf. Fig. 3.6. The permeator tube (Figure 3.8) is named *"Orim 2014 nº5"* and has the following features:

- Effective Pd-Ag length: 152 mm;
- External diameter: 10 mm;
- Wall thickness: 150 μm.

The effective length is related to the length of the membrane where permeation occurs (the Pd-Ag membrane).

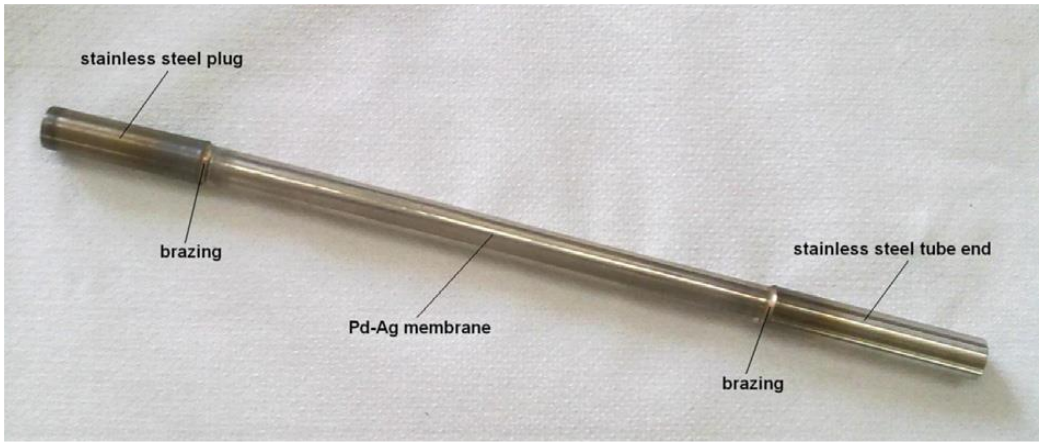

Figure 3.8 – Permeator tube "Orim 2014 nº5".

This permeator tube is closed at one side and connected to a stainless steel to the other one. The feed tube is assembled through this later end, inside the permeator tube, as a "tube in

tube" configuration. The membrane was assembled to the shell in order to allow the elongation of the membrane to one side (reducing the stress of the membrane), with the feeding occurring on the other. As such, the feed stream is fed to the membrane directly into the Swagelok cap, at which point it reverses its direction and flows through the full length of the membrane, which is filled with the catalyst and glass spheres. Consequently, the hydrogen fed/produced is permeated through the membrane to the shell where it is swept with nitrogen (permeate stream). The stream that reaches the end of the membrane, with non-permeated hydrogen and remaining gases, is called "retentate stream". This description can be observed in Figure 3.9 a).

The permeator tube was filled with 12.076 g of catalyst and 12.98 g of inert glass spheres (Glasperlen, 2 mm diameter). The catalyst, produced by the University of Salerno, was a bimetallic one, based on Pt (3 wt.%) and Ni (10 wt.%) and supported on CeO_2.

Figure 3.9 shows a scheme of the membrane reactor and an image of the reactor used in this work.

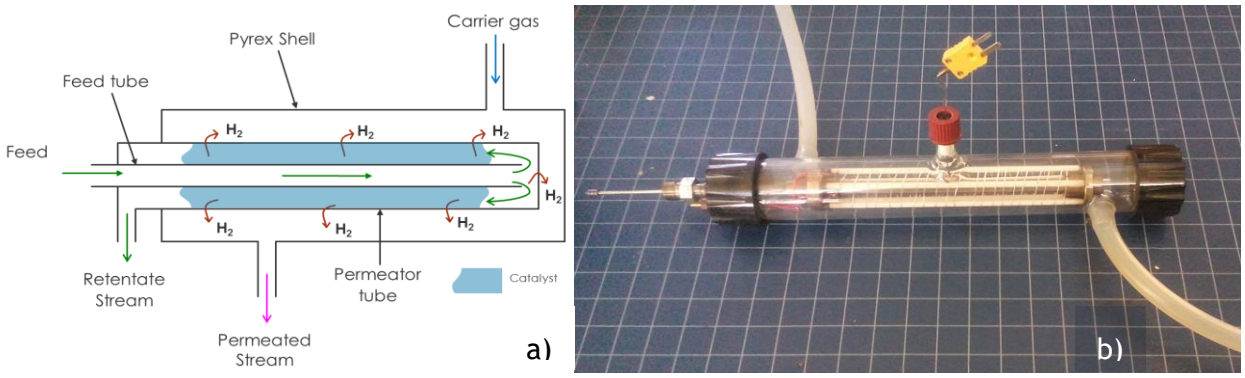

Figure 3.9 – a) scheme of the membrane reactor and b) the membrane reactor used in the present work.

The heating of the membrane, based in the Joule effect, takes place through coils of platinum where DC current circulates. These coils are curled around five circular rods of alumina, placed in a triangle formation with the membrane at its center. The temperature is controlled by a K-type thermocouple (TC), inserted through an opening in the shell, which is placed perpendicular to the membrane, almost touching it.

Two pressure transducers (P2, P3), Baratron® 700 series (Full scale: 5 x 10^5 Pa / Accuracy: 1% F.S. (5 kPa)), measure the pressure in the membrane. They are placed at the entrance of the membrane, in the feed stream, and right after the exit of the retentate side (Fig. 3.6). The specifications for both transducers are the same.

As previously said, the membrane is inserted in a shell of Pyrex glass in a finger-like configuration, which reduces de stress imposed to the membrane. This container has two openings: an entrance for the sweep gas (nitrogen) and an exit for the permeated stream (the permeated hydrogen and the sweep gas). The sweep gas is nitrogen because not only it does not react but also has the same conversion factor as hydrogen, which allows the quantification of the amount of hydrogen permeated by the membrane. The shell is closed at both ends by two bachelite threaded caps, the temperature of which is checked by means of two K-type thermocouples (TC3, TC4) so as not to damage the sealing of the membrane.

The retentate stream is directed to a condenser submerged in a liquid trap. Here, two streams can be obtained. The gas phase, also known as syngas, is mainly constituted of hydrogen, CO_2 and CH_4. This stream is analysed through a gas chromatograph where we are able to discern the amount of hydrogen not permeated through the membrane as well as the amount of methane in the stream, which is an indicator of the activity / selectivity towards the side reactions. With the liquid (condensed) phase we are able to study the phenols content.

Both thermocouples and the pressure transducers referred above are connected to the acquisition and control system, explained in a following section.

As a matter of security, the experimental set up is located inside a ventilated fume hood in order to continually exhaust the gases being released when the membrane is operating.

3.1.6.1 Methanation of Olive Mill Wastewater

Relating to the methane production as an alternative to OMW valorisation, although the existing setup was also used, it was not with a membrane reactor configuration. In fact, hydrogen (now reactant) was fed through the shell side, whose pressure was kept constant at 1 bar by closing the permeate side exit and controlling the flow provided to the set up in the origin (either the hydrogen tank or the hydrogen generator).

Hydrogen is transferred from the shell (permeate side) to the membrane (feed/retentate side) at a rate influenced by the partial pressure difference between the shell and the membrane side and the need imposed by the reaction. Since there are more than one component in the retentate stream, it is necessary to do a chromatography analysis in order to know its composition.

3.1.7 **Permeate Side**

The hydrogen permeated through the membrane in the membrane reactor configuration (i.e., when hydrogen is produced from the OMW) is swept with a stream of nitrogen, which constituted the permeated stream. The amount of nitrogen fed as the sweeping stream is

measured and controlled by the gas mass flow controller "GMFC2" described in the section "3.3.1 Feed".

The flow of permeated stream leaving the shell (permeated hydrogen and nitrogen) is measured by a flowmeter (FM – cf. Fig. 3.6). Since the nitrogen fed to the membrane does not react, it is possible to calculate, by the difference, the amount of hydrogen permeated.

3.1.8 Retentate Side

The retentate stream is mainly composed of non-permeated hydrogen, reagents which did not react and products of side reactions. Leaving the reactor, the stream is directed to a cold trap that functions as a condenser, submerged in a mixture of alcohol and liquid nitrogen.

The retentate stream is divided into a liquid and a gas phase in order to be possible to analyse the gas stream in the gas chromatograph. Before the gas phase being released, a needle valve (NV) regulates the pressure inside the membrane.

1.1.1 Acquisition and control system

The acquisition and control of the process parameters is done using a program built using *LabView* with a *National Instruments* interface run in a personal computer, assembled near the experimental set up. Figure 3.10 shows an image of the used interface.

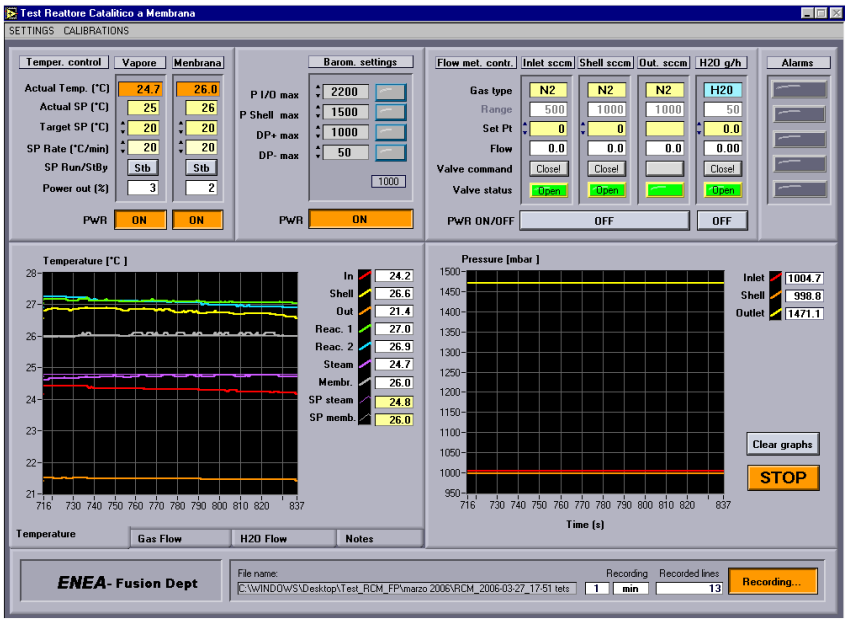

Figure 3.10 – Image of the acquisition and control system.

3.1.9 Gas chromatography

The gas phase sample of the retentate stream was collected using a plastic sample bag (Figure 3.11) for the gas chromatography analysis.

Figure 3.11 – Sample bag used to collect the retentate sample.

Before collecting a sample, the sample gas bag was cleaned using a ventury vacuum pump, connected to a nearby water tap, and flushed with nitrogen. This process was repeated at least two times before collecting the sample. The sample bag has a valve which allows it to be leak proof. In order to allow the gas to flow, the valve must be turned counter-clockwise and, similarly, clockwise to stop the flow.

The gas samples were analysed using a micro-GC *Chrompack* portable "*Micro GC CP-2002*", illustrated in Figure 3.12. The apparatus is equipped with a thermal conductivity detector (TCD) and two analytical columns, *Molsieve 5A* plot and *CP-Cox*, using argon as carrier gas.

Figure 3.12 - Micro-GC Chrompack *portable* "Micro GC CP-2002".

3.2 Experimental Plan

The experimental plan consisted in three phases: characterization of the membrane (through permeation tests), reaction tests for the production of hydrogen and reaction tests for the production of methane. Also, leak tests were performed between each reaction/permeation test in order to guarantee the good physical conditions of the membrane.

Initially, only the reaction tests for the production of hydrogen through steam reforming (SR) were planned as a way to valorise OMW. The plan consisted on studying different feeds of OMW and methane (10 g h^{-1}:10 sccm, 15 g h^{-1}:15 sccm and 20 g h^{-1}:20 sccm) at 450 ºC, increasing and decreasing the pressure inside the membrane. The goal of feeding methane is to further enhance the hydrogen production by reacting the excess water of the OMW, which was not separated during the distillation, with methane (this way the energy spent in vaporizing the feed, with a great amount of water, is not wasted). The tests were performed at 450 ºC because according to previous works, preliminary tests at 400 ºC produced a very negligible amount of hydrogen (Tosti et al., 2013); also, the steam reforming reaction being highly endothermic, is favoured at high temperatures, from the thermodynamic and kinetic point of view. However, temperatures higher than 450 ºC might affect the membrane.

Since the hydrogen production through this method was very slim, another reaction test with a feed composition of OMW/CH_4 of 15 g h^{-1}:15 sccm was performed, this time being the OMW the one from a previous work carried out at ENEA (Presterà, 2014). Still in view of the production of hydrogen, another set of tests was carried out focusing on the oxidative steam reforming (OSR), with both the OMW from this and the referenced previous work. The C/O_2 molar ratio used was 1:4 which consisted on a feed of OMW/O_2 of 15 g h^{-1}:101.5 sccm (the steps to calculate this ratio can be viewed in Appendix 1). The operating temperature and pressure of these tests where identical to the ones applied to the steam reforming reaction.

Since the tests described did not provide positive results, another strategy was adopted for the OMW's valorisation, by studying the production of methane through hydrogenolysis. Before the test with OMW, the hydrogenolysis reaction was tested also with ethanol. These tests were performed at 300 ºC, increasing and decreasing the operating pressure. In the case of ethanol, also tests at each pressure (1, 3 and 5 bar) were performed, with 30 min regeneration between them. Although this approach was never previously executed, thermodynamically speaking it is suggested that the reaction is favoured at lower temperatures, reason why a temperature of 300 ºC was selected to perform this test.

After each set of tests, which took approximately 1-2 h for increasing/decreasing pressures (with about 30 min for a given pressure), the regeneration of the catalyst was performed,

flowing hydrogen for approximately 1 h. Due to coke deposition, the catalyst regeneration is reached through the following reaction:

$$C + 2H_2 \leftrightarrow CH_4 \quad \Delta H = -74.8\ kJ\ mol^{-1} \tag{3.1}$$

In Table 3.3 is summarized the experimental work performed.

Table 3.3 - Summary of the experimental work.

Test	Feed	Composition	T / P
Control	H_2O (g h^{-1}) / CH_4 (sccm)	15:15	450 ºC 1 – 3 – 5 bar 5 – 3 – 1 bar
	OMW (g h^{-1}) / N_2 (sccm)	15:15	
Steam reforming	OMW (g h^{-1}) / CH_4 (sccm)	10:10 15:15	
	Previous OMW (g h^{-1}) / CH_4 (sccm)	15:15	
Oxidative Steam Reforming	OMW (g h^{-1}) / O_2 (sccm)	15:101.5	
	Previous OMW (g h^{-1}) / O_2 (sccm)	15: 101.5	
Hydrogenolysis	EtOH (96% v/v) (g h^{-1})	15	300 ºC 1 – 3 – 5 bar 5 – 3 – 1 bar 1 – R – 3 - R - 5 bar
	EtOH (10% v/v) (g h^{-1})	15	300 ºC 1 – 3 – 5 bar 5 – 3 – 1 bar
	OMW (g h^{-1})	15	

In the following sections are the procedures for all the tests performed throughout the experimental work: permeation tests, steam reforming tests, oxidative steam reforming tests and hydrogenolysis tests.

3.2.1 Permeation Test

1. Turn on the exhaustion system of the hood. Run the acquisition and control program and push the recording button. Insert the values of temperature and flow desired;
2. Start heating the membrane with a rate of 10 ºC min^{-1} until the desired temperature (300, 350, 400, 450 ºC) flowing 200 sccm of N_2, both through the shell and membrane;
3. When the temperature is reached, change the flow of N_2 to H_2, the same flow rate, inside the membrane;
4. Increase the pressure inside the membrane with the needle valve (NV), as desired (1 - 5 bar);
5. After finishing the tests, cease flowing H_2, replacing it with N_2. Decrease the temperature by setting it to 0 ºC with a rate of 60 ºC min^{-1};

6. When the temperature reaches ambient temperature, switch off the heating system and pressurize the membrane for the leak test.

3.2.2 Oxidative Steam Reforming and Steam Reforming Test

1. Repeat steps 1 and 2 from the Permeation Test;
2. Fill the liquid tank with the amount of liquid necessary for the test;
3. Start heating the vaporizer heating system to 200 ºC with a heating rate of 10 ºC min^{-1};
4. When the temperature is reached, change the flow of N_2 to H_2 (same flow rate), inside the membrane, for approximately 15 min in order to eliminate possible residues of coke from a previous test;
5. Following, change back the flow to N_2 for 5 min to remove any H_2 and turn on the liquid mass flow meter (LMFM);
6. Set the flow of liquid (OMW or ethanol), leaving it for 15 min in order to stabilize the LMFM;
7. Change the N_2 to CH_4 (or O_2, in case of the OSR), in the amount required to perform the test;
8. Approximately 30 min after starting the test take a sample for the chromatography analysis;
9. Increase the pressure inside the membrane with the needle valve (NV), as desired (1, 3 or 5 bar), repeating then step 8;
10. After finishing the test, stop the flow of liquid and change the CH_4 to H_2 and collect the liquid inside the condenser;
11. Decrease the pressure to 1 bar and flow hydrogen for approximately 1 h to regenerate the catalyst (by reacting the coke with hydrogen forming methane);
12. After the regeneration, continue with steps 5 and 6 of the Permeation test.

3.2.3 Hydrogenolysis Test

1. Repeat steps 1 to 6 of the previous test;
2. Change the flow of N_2 to H_2 entering the shell on the GMFM2 setting a flow of 500 sccm (maximum flow). Close the valve at the exit of shell and adjust the flow being produced in the H_2 generator to stabilize the pressure inside the membrane at 1 bar;
3. Set the N_2 entering the membrane to 200 sccm;

4. Approximately 30 min after starting the test take a sample for the chromatography analysis;
5. Increase the pressure inside the membrane with the needle valve (NV), as desired (1, 3 or 5 bar), repeating step 4;
6. After finishing the test, stop the flow of liquid and change the H_2 on the shell to N_2,the flow of N_2 entering the membrane to H_2 and collect the liquid inside the condenser;
7. Decrease the pressure to 1 bar and flow hydrogen for approximately 1 h to regenerate the catalyst (by reacting the coke with hydrogen forming methane);
8. After the regeneration, continue with steps 5 and 6 of the Permeation test.

4. Results and Discussion

For organization purposes, this chapter is divided in the following sections:

- Permeation Tests
- Steam Reforming Tests
- Oxidative Steam Reforming Tests
- Hydrogenolysis Tests

4.1 Permeation tests

The membrane was characterized in terms of hydrogen permeability and selectivity, i.e. the ability to diffuse hydrogen throughout the membrane's metal lattice. To execute this test, 500 sccm of pure hydrogen were flushed into the lumen with a constant carrier gas (N_2) flow rate of 200 sccm in the shell. It was performed at different temperatures (300, 350, 400 and 450 ºC) and pressures (1, 2, 3, 4 and 5 bar).

The tests were performed according to the procedure described in Chapter 3.3. As mentioned in Chapter 2, the permeation of hydrogen through a dense palladium membrane can be described by the Sieverts' Law (Equation 2.4).

According to Pérez et al. (2015), by considering the analogy between mass and heat transfer, the temperature driving force of a heat exchanger can be used similarly to describe the hydrogen permeation driving force in the membrane tube:

$$J = \frac{P_e}{\delta}.\Delta P_{ln} \tag{4.1}$$

where ΔP_{ln} is

$$\Delta P_{ln} = \frac{({P_{H_2,in}}^{0.5} - {P_{H_2,p}}^{0.5}) - ({P_{H_2,r}}^{0.5} - {P_{H_2,shell\ in}}^{0.5})}{\mathrm{A}}, \quad A = \ln\left(\frac{{P_{H_2,in}}^{0.5} - {P_{H_2,p}}^{0.5}}{{P_{H_2,r}}^{0.5} - {P_{H_2,shell\ in}}^{0.5}}\right) \tag{4.2}$$

$P_{H_2,in}$ and $P_{H_2,shell\ in}$ are the hydrogen partial pressures in the feed stream and in the stream entering the shell, respectively, while $P_{H_2,r}$ and $P_{H_2,p}$ are the hydrogen partial pressured in the retentate and the permeate streams.

Being that pure hydrogen is fed to the membrane and the pressure drop on the lumen side can be neglected, the hydrogen partial pressure in the retentate side ($P_{H_2,r}$) can be considered constant and equal to the feed pressure ($P_{H_2,in}$). However, this does not occur in the permeate side. Here, the hydrogen partial pressure increases along the tube axis proportionately to the

permeation of hydrogen. The feed entering the shell side is composed in its entirety of nitrogen, reason why the hydrogen partial pressure in said stream ($P_{H_2,shell\ in}$) is zero. According to this, the permeation of hydrogen through the dense palladium membrane can be described instead as:

$$J = \frac{P_e}{\delta} \cdot \frac{{P_{H_2,p}}^{0.5}}{\ln\left(\frac{{P_{H_2,in}}^{0.5}}{{P_{H_2,in}}^{0.5} - {P_{H_2,p}}^{0.5}}\right)} \tag{4.3}$$

where δ is the membrane thickness, $P_{H_2,in}$ and $P_{H_2,p}$ are the hydrogen partial pressures on the feed stream and on the exit permeate side (where N_2 flows in counter-current mode), respectively, and P_e is the permeability coefficient (mol m^{-1} s^{-1} $Pa^{-0.5}$).

As mentioned in Chapter 2, permeation is a thermal process which can be described by the Arrhenius' law:

$$P_e = P_{e,0} e^{\left(\frac{-E_a}{R.T}\right)} \tag{2.6}$$

being $P_{e,0}$ (mol m^{-1} s^{-1} $Pa^{-0.5}$) the pre-exponential permeability coefficient, E_a (J mol^{-1}) the activation energy, *R* the ideal gases constant (8.314 J mol^{-1} K^{-1}) and *T* the absolute temperature (K). Therefore, the values of the pre-exponential permeability coefficient and the activation energy can be obtained from the linear regression:

$$\ln(P_e) = \ln(P_{e,0}) - \frac{E_a}{R} \cdot \frac{1}{T} \tag{4.4}$$

Figure 4.1 shows the results obtained in the permeation tests in the form of hydrogen flow permeated through the membrane vs. hydrogen partial pressure ($P_{H_2,in}$) in the feed stream, for each temperature the permeation test was operated at.

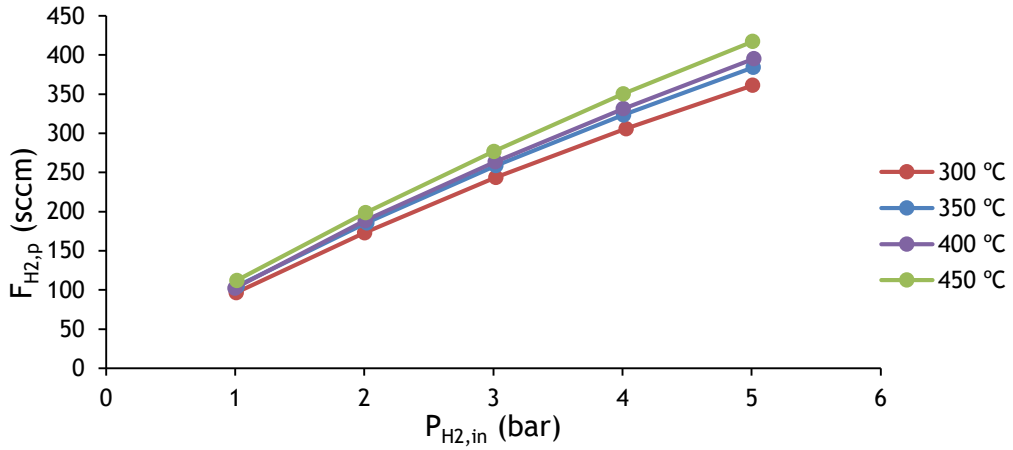

Figure 4.1 – Flow of hydrogen permeated through the membrane with pressure for each operating temperature used.

The behaviour shown in Figure 4.1 is consistent with the theory since it increases with both the operating temperature and pressure.

Table 4.1 exhibits the permeability results obtained using by fitting Equation 4.3 to the experimental data.

Table 4.1 - Permeability results for different temperatures and pressures.

P (bar)	300 ºC	350 ºC	400 ºC	450 ºC
	P_e (mol m^{-1} s^{-1} Pa$^{-0.5}$)			
1	1.02x10^{-8}	1.12x10^{-8}	1.09x10^{-8}	1.21x10^{-8}
2	1.19x10^{-8}	1.28x10^{-8}	1.30x10^{-8}	1.38x10^{-8}
3	1.25x10^{-8}	1.32x10^{-8}	1.32x10^{-8}	1.41x10^{-8}
4	1.37x10^{-8}	1.46x10^{-8}	1.49x10^{-8}	1.59x10^{-8}
5	1.42x10^{-8}	1.51x10^{-8}	1.56x10^{-8}	1.65x10^{-8}

As can be noted, the permeability increases when increasing the total pressure. Also, in general, the permeability increases with the temperature. In Figure 4.2, the graph $\ln(P_e)$ versus $1/T$ reports the linear regression of the permeability results (Arrhenius plot), with the coefficient of determination of each linear regression.

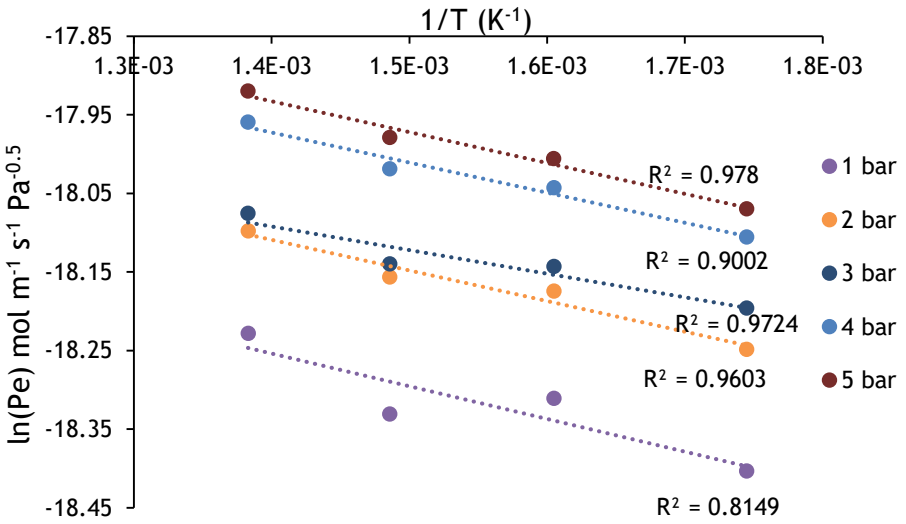

Figure 4.2 - Plot of $ln(P_e)$ vs. $1/T$.

Figure 4.2 allows the calculation of the pre-exponential permeability coefficient and the activation energy, which take the values reported in Table 4.2

Table 4.2 - Results of $P_{e,0}$ and E_a.

P (bar)	E_a (J mol^{-1})	$P_{e,0}$ (mol m^{-1} s^{-1} Pa$^{-0.5}$)
1	3469	$2.12\text{x}10^{-8}$
2	3244	$2.36\text{x}10^{-8}$
3	2498	$2.12\text{x}10^{-8}$
4	3184	$2.68\text{x}10^{-8}$
5	3272	$2.83\text{x}10^{-8}$

Table 4.3 presents published results of E_a and $P_{e,0}$, specified with the operating pressure and temperature range of the related tests, as well as the tested membrane's thickness.

Table 4.3 - Previously published results $P_{e,0}$ and E_a.

δ (μm)	E_a (J mol^{-1})	$P_{e,0}$ (mol m^{-1} s^{-1} Pa$^{-0.5}$)	T range (ºC)	P range (bar)	
143	2106.80	$2.36\text{x}10^{-8}$	400-450	1 – 1.5	Tosti et al. (2015)
200	2592.56	$2.06\text{x}10^{-8}$	200-450	2 - 8	Vadrucci et al. (2013)

The results obtained in this work ($\delta = 150\ \mu m$) are in line with the ones reported above, except for low temperature ranges. The difference in the membrane thickness and the temperature and pressure range can be responsible for some deviations.

4.2 Steam Reforming tests

Three types of steam reforming tests were performed, according to the feed: two control tests (H_2O + CH_4 and OMW + N_2) and OMW + CH_4. As explained in Chapter 3, CH_4 is added in order to react with the remaining water present in the OMW, which was not removed during distillation. These tests were operated at 450 ºC and two sets of pressure rounds were performed: increasing the pressure, from 1, 3 and then 5 bar, and decreasing the pressure (5, 3 and 1 bar), with a regeneration between each round. Figure 4.2 shows a scheme of the membrane reactor during these tests.

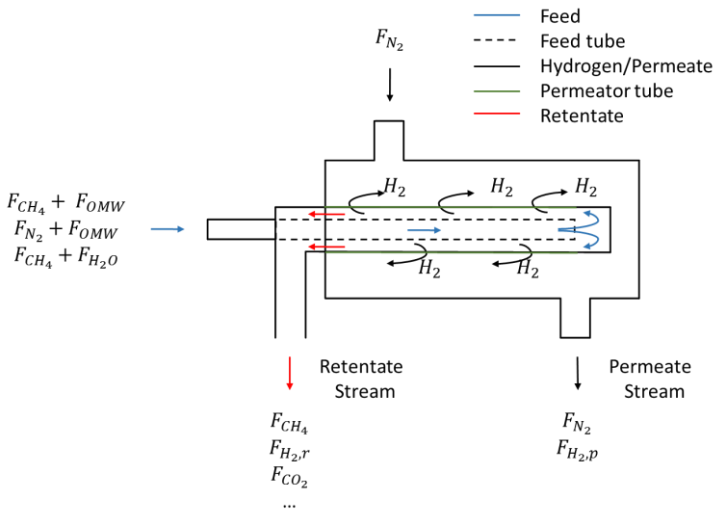

Figure 4.3 - Scheme of the membrane reactor in the steam reforming tests.

The parameter used to evaluate the performance obtained during these tests is the amount of hydrogen produced in the permeate ($F_{H_2,p}$).

The flow of hydrogen permeated is equal to the flow accounted by the flowmeter (FM) (cf. - Figure 3.6) in the permeate stream once removed the flow of nitrogen fed to the shell:

$$F_{H_2,p} = F_{out} - F_{N_2} \tag{4.5}$$

F_{out} (sccm) is the flow measured by the flowmeter and corresponds to the flow of hydrogen permeated plus the flow of nitrogen used as a carrier gas, F_{N_2} (sccm). The amount of nitrogen fed to the shell is the same exiting because nitrogen does not permeate through the membrane.

In the retentate stream it is expected to find CH_4, non-permeated H_2, CO_2, CO and other species originated from the side reactions. Although this stream was expected to be analysed by the gas chromatograph, due to technical problems this analysis was not conducted.

4.2.1 OMW + CH_4 tests

These tests consisted on sending OMW and CH_4 into the membrane reactor feed, which was at 450 ºC, varying the total pressure. First the pressure was increased from 1, then 3 and finally 5 bar and after a regeneration had been done, it was decreased from 5, 3 and 1 bar. The flow fed to the membrane in two different runs is specified in Table 4.4.

Table 4.4 - Flow of OMW and CH_4 fed to the membrane.

F_{OMW} (g h^{-1})	F_{CH_4} (sccm)
15	15
10	10

The gas flow rates indicated refer to standard conditions (atmospheric pressure and 0 ºC of temperature).

The results obtained are plotted in Figure 4.4 as $F_{H_2,p}$ vs. *Total Pressure*.

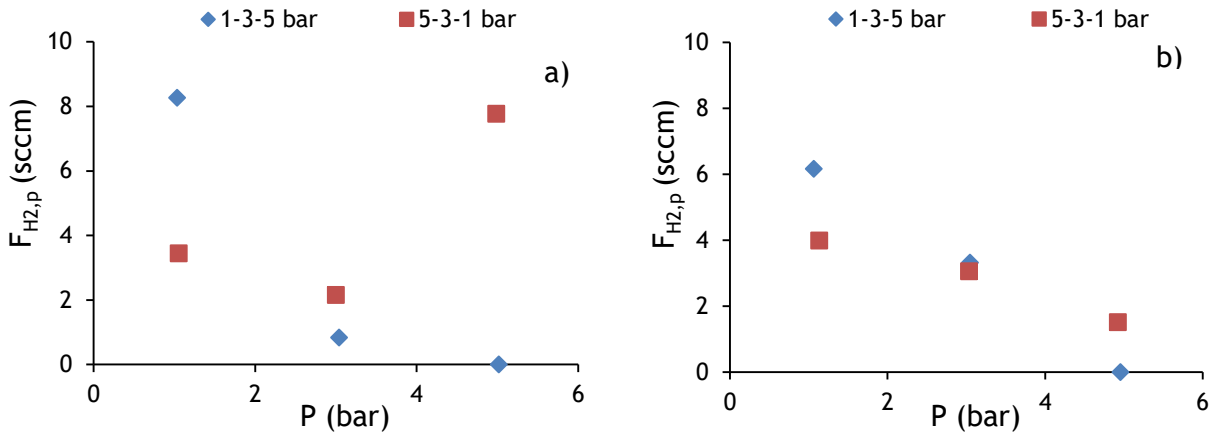

Figure 4.4 - Results obtained during the steam reforming tests with a feed of CH_4 and OMW, with different flow rates: a) 10 sccm and 10 g h^{-1} and b) 15 sccm and 15 g h^{-1} for CH_4 and OMW, respectively.

As observed in Figure 4.4, generally the amount of hydrogen produced decreases with pressure, with a point in Figure 4.4 a), at 5 bar during the "5 – 3 - 1 bar" pressure set, deviating from the norm.

Particularly for Figure 4.4 b), it is well observed the effect of the catalyst deactivation on the flow of hydrogen permeated. At 5 bar, the amount of hydrogen permeated in the pressure set "5 – 3 - 1 bar", after a regeneration, is higher than the hydrogen permeated at the end of the test "1 – 3 – 5 bar". Also, at 1 bar, the hydrogen permeated at the end of the "5 – 3 - 1 bar" test is lower than the value obtained at the beginning of the test "1 – 3 – 5 bar".

The accuracy of the measured values by the flowmeter was calculated in order to evaluate their admissibility. Equation 4.7, included in the flowmeter's specifications, was used to that effect.

$$Accuracy = 0.2\%.\,Full\ Scale + 0.5\%.\,Read\ Value \tag{4.6}$$

It was found that the $\%Accuracy/Read\ Value$ ranged from approximately 12.5% to 100%. These results lead us to conclude that the magnitude of the collected values was judged too close to the sensitivity of the flowmeter.

The water collected from the condenser was analysed in terms of phenols content. The results performed by the University of Naples, with the method described in Chapter 3, are reported in Table 4.5. The temperature at which the tests were performed was 25 ºC.

Table 4.5 - Chemical analysis of the treated OMW

Sample	pH	Total Phenols (mg L^{-1})
OMW + CH4 10 sccm	4.17	23.4
OMW + CH4 15 sccm	3.96	45.8

In order to understand if the problems that occurred during distillation had effect in the production of hydrogen, a test with the OMW from a previous work (Presterà, 2014) was performed. The test was conducted by feeding 15 sccm of CH_4 and 15 g h^{-1} of OMW using the same operating conditions. Said test was also compared with the results of a previous experiment where 15 sccm of CH_4 and 15 g h^{-1} of OMW were fed to the membrane (Presterà, 2014). This one was filled with 5.016 g of a Rh/Pt washcoat catalyst and the temperature and pressure conditions remained the same. In Figure 4.5 are represented the results obtained as well as the ones from the previous work.

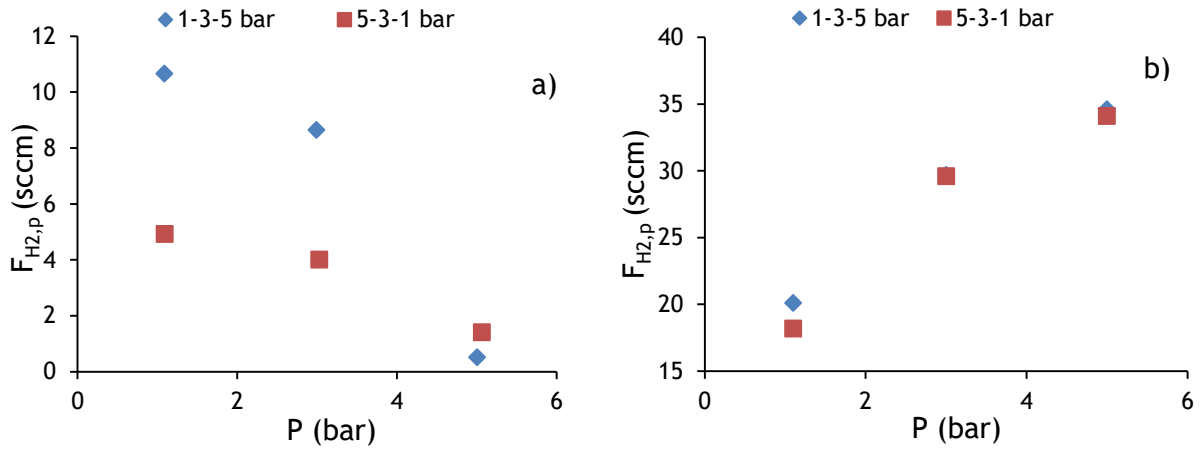

Figure 4.5 - Steam reforming tests results obtained using a previous OMW a) on the present experiment and b) by Presterà (2014), with a Rh/Pt washcoat catalyst.

As can be observed, the amount of hydrogen produced with a previous OMW (Figure 4.5 a)) and the Ni/Pt based catalyst is slightly higher than with the OMW shown in Figure 4.4 (also with the Ni/Pt based catalyst). This indicates that although the distillation might have had some effect in the results, it was not substantial, seeing that they are still very close to the sensitivity of the instrument. However, when compared with the results from the previous experiment by

Presterà (2014), the amount of hydrogen produced is less than 33%. It should also be noted that the pressure should affect the process in three factors. From the thermodynamic point of view, because the reaction takes place with an increasing on the number of moles, it is promoted at lower pressures. Furthermore, according to the Sieverts' law, the increase of pressure moves in favour of the permeation of hydrogen (through the increase of the permeation's driving force). Finally, an increase of pressure also increases the reaction kinetics As such, in the previous work by Presterà (2014) there was a noticeable dominion of the permeation and kinetics over the thermodynamics of the reaction which favoured the production of hydrogen, a fact that was not observed during this work. Both these reasons could indicate an infectivity of the catalyst now used towards the steam reforming reaction.

4.2.2 Control tests

As previously stated, two different control tests were performed. On one test, 15 g h^{-1} of H_2O and 15 sccm of CH_4 were fed to the membrane. It was conducted at 450 ºC and the pressure was increased (1, 3, and 5 bar) and decreased (5, 3 and 1 bar) with a regeneration between each set. The aim of this test was to compare the production of hydrogen by methane steam reforming with the test with the OMW + CH_4.

The second test was performed by feeding 15 g h^{-1} of OMW and 15 sccm of N_2 to the membrane reactor, with the operating conditions of the test being equal to the CH_4/H_2O test. Figure 4.6 shows the results for the H_2O and CH_4 test.

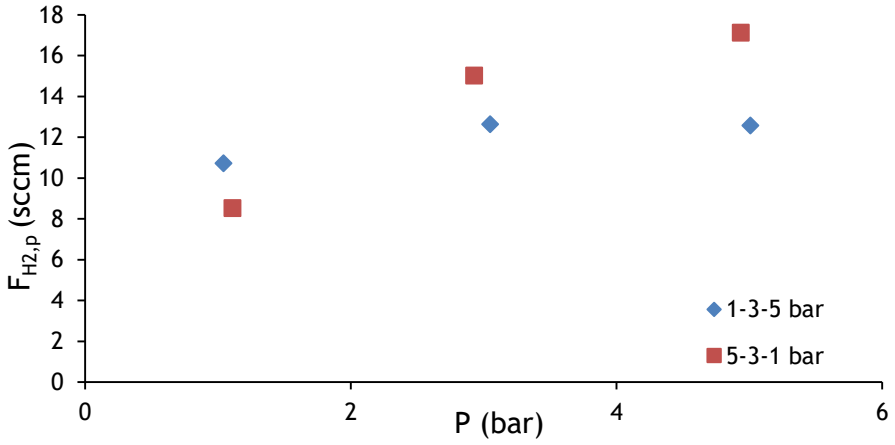

Figure 4.6 - Results of the H_2O and CH_4 steam reforming control test.

The production of hydrogen was still very low for both of these tests, although it was especially low on the test with OMW/N_2 (data not shown). The results for the second tests are below the

instrument sensitivity, reason why they are not presented here. The percentage of the instrument error in the test of H_2O and CH_4 is of approximately 10%.

With respect to the test of H_2O and CH_4 there is a discrepancy on the effect of pressure as compliant with Figures 4.3 and 4.4 a). According to the pressure effect described above, the results show a possible dominant effect of the permeation of hydrogen (shift effect) and reaction kinetics that overcomes the thermodynamics. Catalyst deactivation probably also occurred as evidenced by the results obtained.

Because of the low acceptability of these results, particularly when OMW is present in the feed the steam reforming tests were abandoned and a different approach towards the valorisation of the OMW via production of hydrogen was followed by testing the catalyst used herein (3 wt.% Pt / 10 wt.% Ni / CeO_2) for the oxidative steam reforming.

4.3 Oxidative Steam Reforming

The oxidative steam reforming test was performed by feeding 15 g h^{-1} of OMW and 101.5 sccm of O_2 inside the membrane, according to the scheme represented in Figure 4.7.

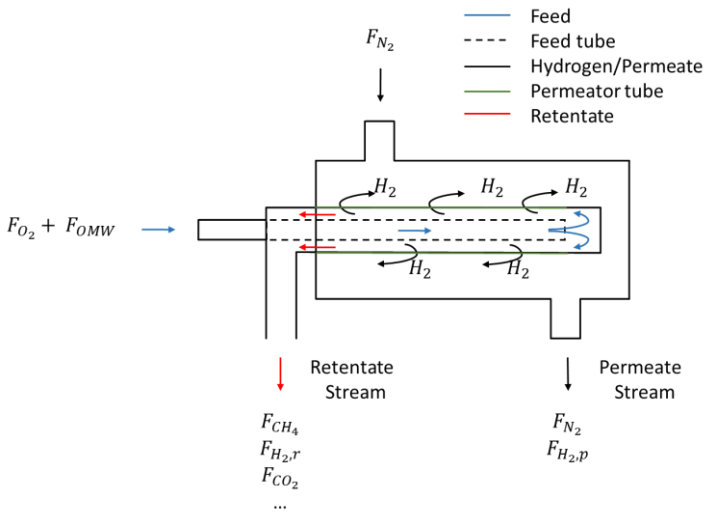

Figure 4.7 – Scheme of the oxidative steam reforming test

The flow of O_2 was calculated according to a molar ratio of 4 moles of carbon to 1 of O_2 (Appendix 1). The test was performed at 450 °C, with two sets of pressure rounds: "1 – 3 – 5 bar" and "5 - 3 - 1 bar", with a regeneration between each set.

The hydrogen production for this test was null. Later after this work, an analysis of the OMW showed that the TOC used to calculate the C/O_2 ratio was different than the one assumed (based on Tosti et al. (2015) work), which means that the actual ratio used was of 1 mole of C to 2 of O_2. This excess of oxygen used could be responsible for the null production of hydrogen from this reaction.

Since the catalyst did not perform well in the tests for the production of hydrogen, the experience continued in terms of valorisation of OMW, still with the present catalyst (3 wt.% Pt / 10 wt.% Ni / CeO_2), in order to produce methane.

4.4 Hydrogenolysis tests

As explained in Chapter 3.2, the set up previously used was slightly changed in order to perform these tests. 15 g h^{-1} of OMW (or ethanol 10% or 96 % v/v) and 15 sccm of N_2 as a carrier gas were fed inside the membrane. The shell, full with hydrogen at 1 bar, was closed at the exit (the "permeate" side) and the pressure out of the hydrogen generator was adjusted in order to meet the specified shell pressure (1 bar). The tests were performed at 300 ºC and at various pressure rounds in the membrane. These pressure rounds, described in the following sections, relate to the pressure inside the membrane. Figure 4.8 is a scheme of this set-up.

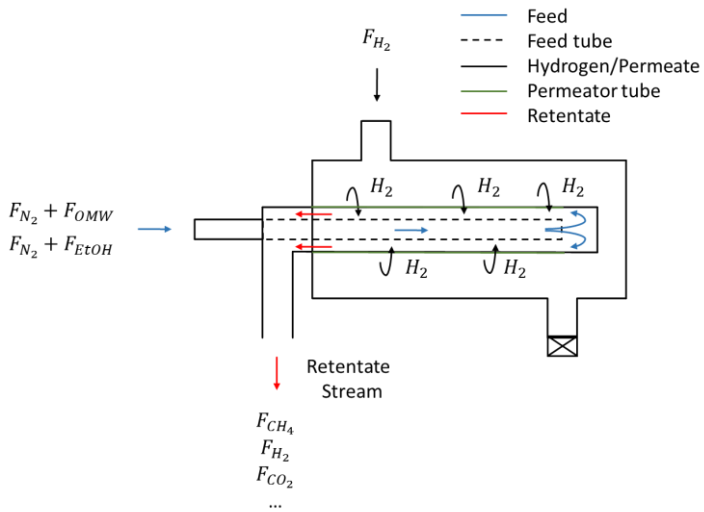

Figure 4.8 – Scheme of the hydrogenolysis test

The "retentate" stream was analysed using a gas chromatograph and the results of the tests were evaluated with the methane yield:

$$Y_{CH_4}(\%) = \frac{F_{CH_4}}{2F_{EtOH}} \times 100$$

Methane yield is a function of the flow of methane produced per flow of ethanol fed to the membrane. The factor 2 is related to the reaction's stoichiometry.

Following are explained the results of the experiences with ethanol 96% v/v (H_2/C ratio of approximately 0.6), ethanol 10% v/v (H_2/C ratio between 7 and 12, according to the operating pressure) and OMW.

4.4.1 Test with EtOH (96% v/v)

This test was performed by feeding 15 g h^{-1} of EtOH (96% v/v), which corresponds to approximately a H_2/EtOH ratio of 0.6. This ratio value was calculated with the amount of hydrogen fed to the membrane and measured by the GMFM2 (cf. – Figure 3.7). It was done for three sets of pressure (inside the membrane): increasing the pressure (1 - 3 - 5 bar) and decreasing the pressure (5 - 3 - 1 bar), with a regeneration between them, and increasing the pressure with regeneration between each pressure (1 – R – 3 – R – 5 bar). The operating temperature was 300 ºC.

The chromatographic analysis of the final stream of this tests showed presence of CH_4, non-reacted hydrogen, carbon dioxide and carbon monoxide, besides the nitrogen stream which does not react.

The test of pressure decrease (5 - 3 - 1 bar) conducted abnormally when compared to the other set of tests reason why it will not be taken in consideration. The results obtained are shown in Figure 4.9.

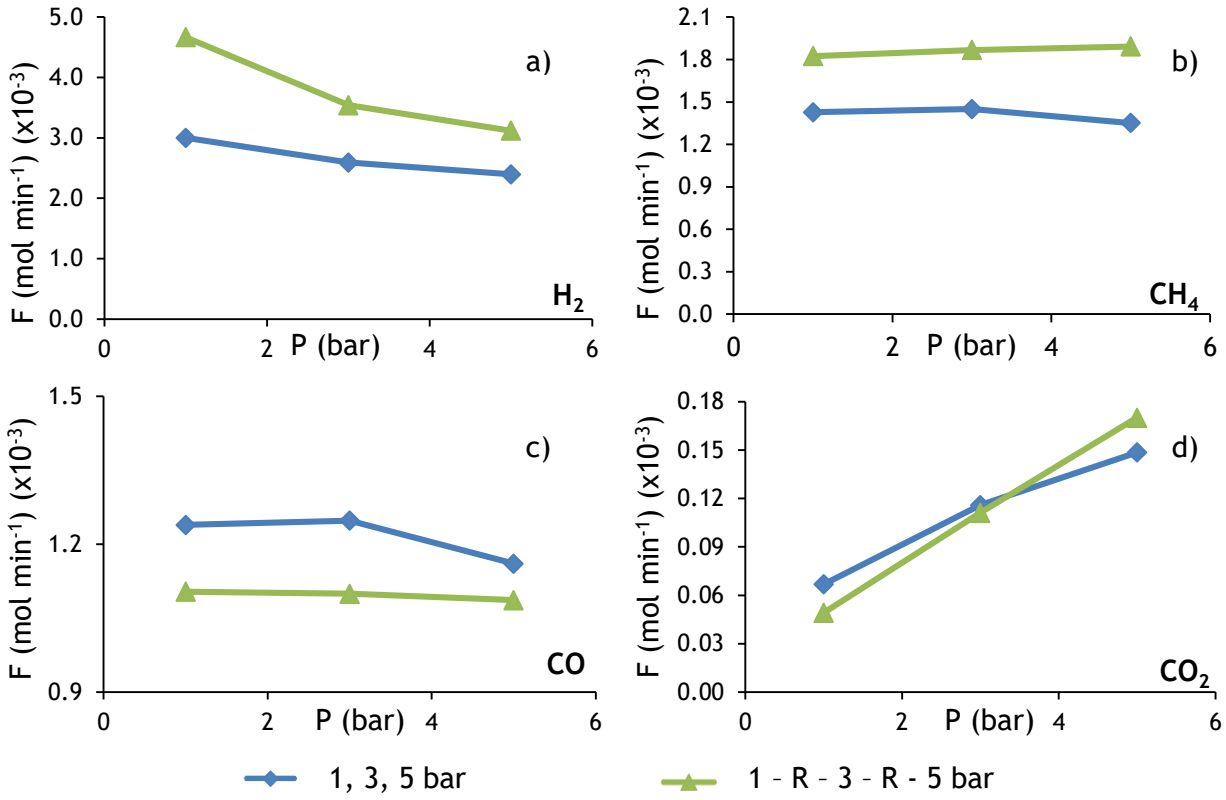

Figure 4.9 – Behaviour of a) hydrogen, b) methane, c) carbon monoxide and d) carbon dioxide in the retentate stream with pressure during the hydrogenolysis of EtOH (96% v/v).

The liquid on the condenser, recovered after each test, had a very high amount of coke deposit. This deposit was in much higher quantities than in the previous experiments (for the production of hydrogen), during approximately the same time of testing, as it was clearly noticeable in the liquid. Thus, the catalyst could require a much larger regeneration time and an increase in the reaction temperature (since the coke formation reactions are favoured at lower temperatures).

The only difference between sets of pressure tests is the regeneration performed between each pressure in the case of the "1 – R - 3 - R - 5 bar". As such, at 1 bar the results should be equal, which is not observed.

In the case of hydrogen (Figure 4.9 a)), it is evidenced with the increase of pressure a consequent drop in the amount of hydrogen in the retentate stream, for both tests. In a normal membrane reactor, an increase of pressure in the membrane should increase the permeation of hydrogen. But in this case, the movement of hydrogen is from the shell to the membrane, which means that an increase of the pressure on the membrane side would decrease the permeation (contrary to increasing the pressure on the shell side).

A slight increase of methane with pressure is observed in Figure 4.9 b). Although thermodynamically speaking, the reaction is not favoured with the increase of pressure, the

rate of the reaction should be favoured by an increase of pressure, which could explain the phenomenon observed.

The pressure increase test shows a drop on the catalyst activity observed at the end of the pressure set "1 – 3 – 5 bar", where there is a drop in methane production. This is corroborated by the decrease of the production of methane and carbon monoxide (Figure 4.9 b) and c), respectively), when compared to the test with regeneration. The increase in CO_2 presence could be due to the production of coke by the Boudouard reaction.

In Table 4.6 are included the methane yield results and in Figure 4.10 is plotted the variation of the methane yield with the pressure.

Table 4.6 – Percentage of methane yield obtained for the test with EtOH (96% v/v).

Pressure (bar)	CH_4 Yield (%)	
	1 – 3 – 5 bar	1 – R – 3 – R – 5 bar
1	13.70	17.51
3	13.92	17.92
5	12.97	18.16

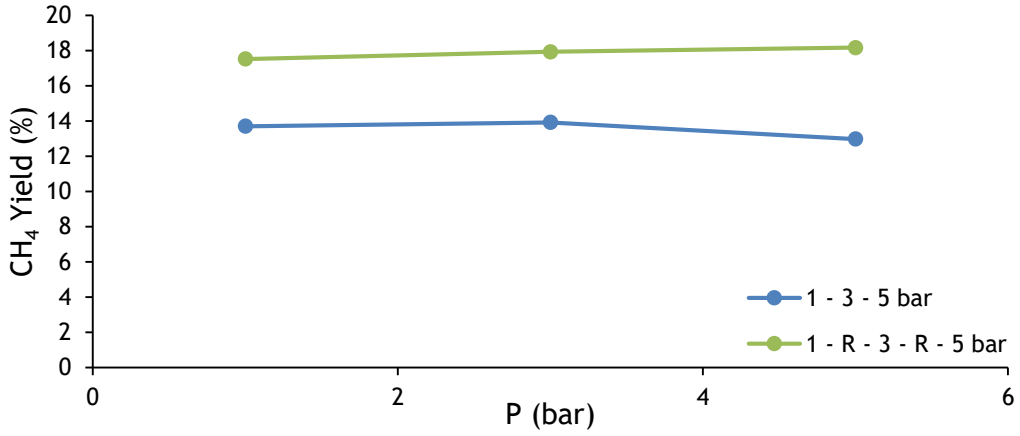

Figure 4.10 – Variation of the methane yield with pressure for the hydrogenolysis of EtOH (96% v/v).

As expected, and referred above, the pressure should not affect positively the hydrogenolysis reaction from the thermodynamic point of view, but it could have an effect in the rate of the reaction, translated in an increase of the methane produced, observed in Figure 4.10. The test with the pressure increase without regeneration has a drop in the hydrogen yield between pressures 3 and 5 due to coke deposition. The maximum yield of methane obtained is 18.16%.

4.4.2 Test with EtOH (10%)

In order to test this reaction with a higher H_2/EtOH ratio (between 12 at 1 bar and 7 at 5 bar, according to the hydrogen permeated), the test was performed with ethanol in a concentration of 10% v/v. The tests were operated at a temperature of 300 ºC with two sets of pressure rounds (related to the membrane side): increasing the pressure (1 - 3 - 5 bar) and decreasing the pressure (5 - 3 - 1 bar), with a regeneration between them.

The results are reported in Figure 4.11.

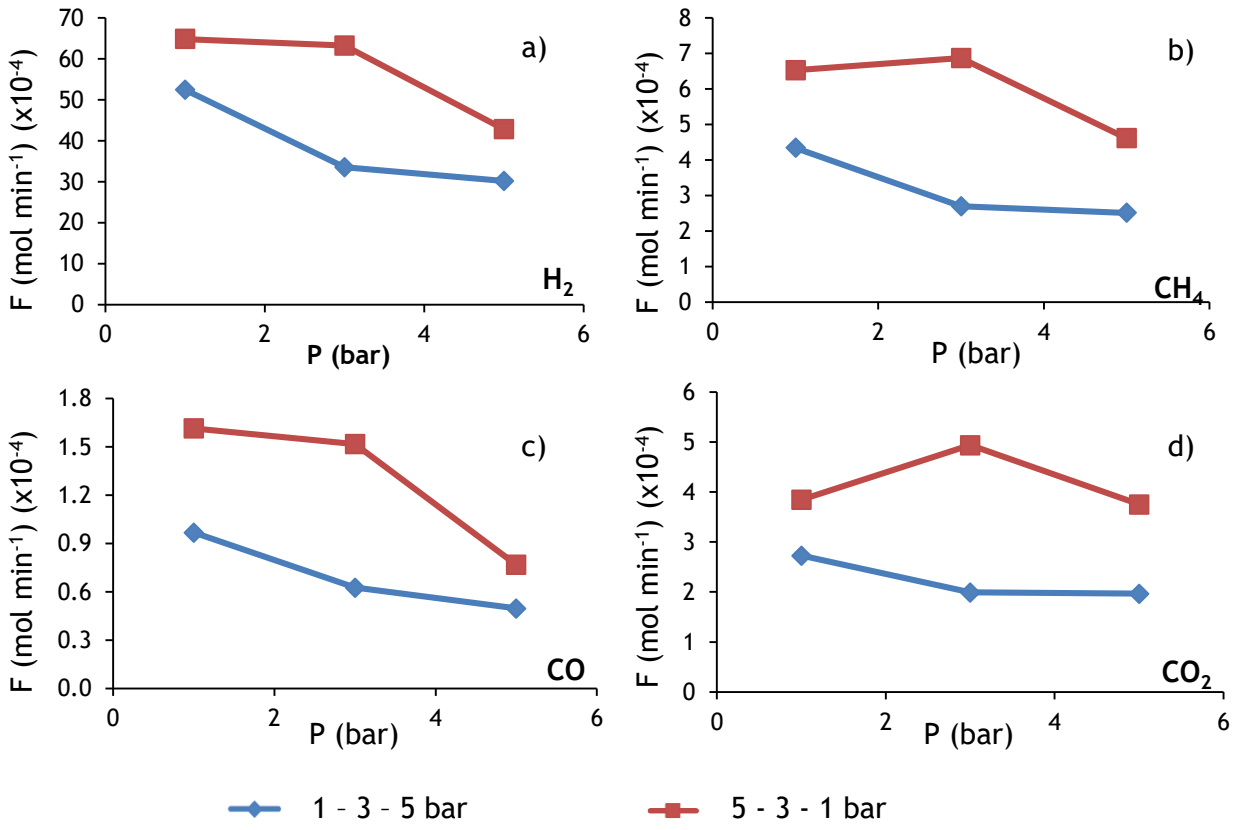

Figure 4.11 - Behaviour of a) hydrogen, b) methane, c) carbon monoxide and d) carbon dioxide in the retentate stream with pressure during the hydrogenolysis of EtOH (10% v/v).

In the case of hydrogen presence in the stream, Figure 4.11 a) shows that it decreases with the increase of pressure, as explained in the previous section.

The coke deposition is noticeable particularly for the CH_4 behaviour (Figure 4.11 b)) where the production at the end of the "1 - 3 - 5 bar" test remains constant improves after regeneration at 5 bar and then in the test decreasing the pressure it even drops at 1 bar. The behaviour observed on the CO and CO_2 part (Figure 4.11 c) and d), respectively) seem to be directly related to CH_4.

The regeneration of this test seemed enough to remove the coke deposited during the reaction since at 5 bar the methane produced in the "5 - 3 – 1 bar" pressure test is higher that the increase of pressure test. This is probably due to the lower percentage of ethanol, which migh be translated in less coke produced.

The methane yield results can be observed in Table 4.7.

Table 4.7 – Percentage of methane yield obtained for the test with EtOH (10% v/v).

Pressure	1 - 3 - 5 bar	5 - 3 - 1 bar
1	40.01	60.13
3	24.87	63.31
5	23.16	42.48

In Figure 4.12 is plotted the methane yield obtained in this test.

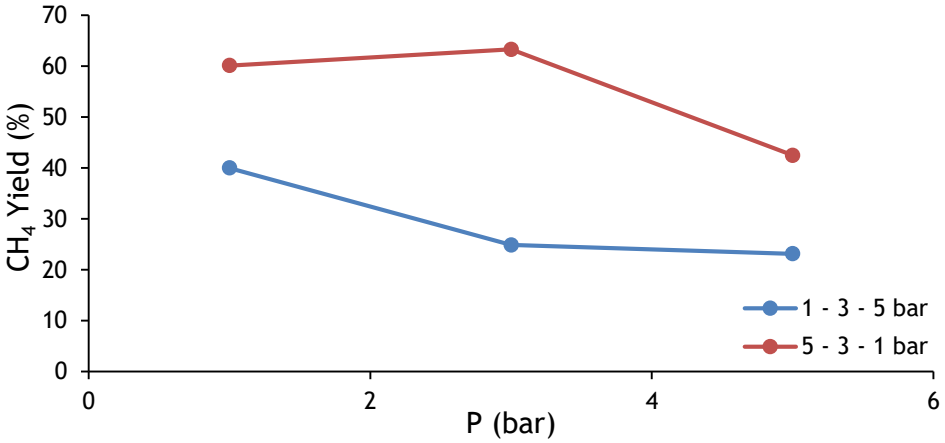

Figure 4.12 - Variation of the methane yield with pressure for the hydrogenolysis of EtOH (10% v/v).

The increase of the H_2/EtOH ratio substancially increases the methane yield from a maximum of 18%, on the previous test (with 96% v/v EtOH), to 63.3%.

4.4.3 Olive Mill Wastewatwer

This test was performed by feeding 15 g h^{-1} of OMW to the membrane, in the same operating conditions as the other two tests and for two sets of pressure: increasing (1, 3 and 5 bar) and decreasing (5, 3 and 1 bar), with a regeneration between each round. The results for the

behaviour of hydrogen, methane, carbon monoxide and carbon dioxide are shown in Figure 4.13.

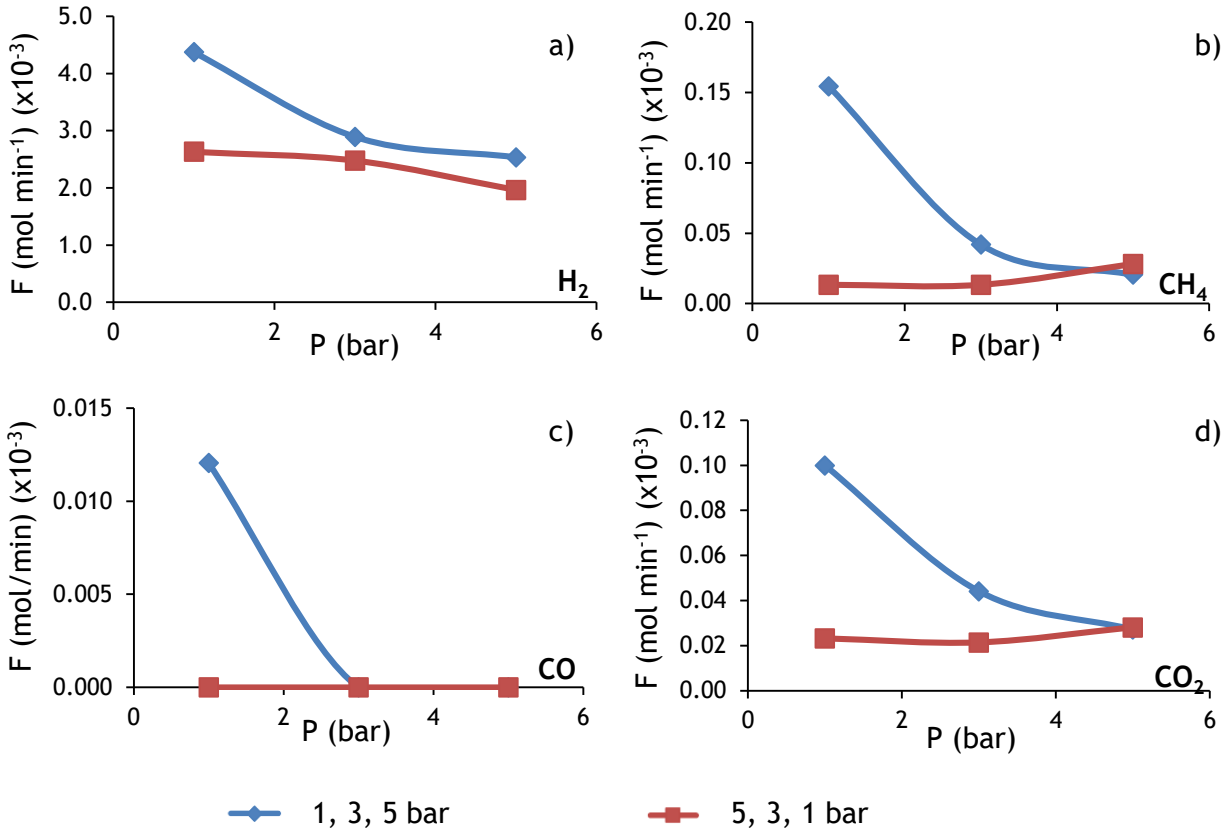

Figure 4.13 - Behaviour of a) hydrogen, b) methane, c) carbon monoxide and d) carbon dioxide with pressure during the hydrogenolysis of OMW.

The hydrogen behaviour is in line with the previous results, generally decreasing with the pressure. From the methane, carbon monoxide and carbon dioxide behaviours (Figures 4.13-b), c) and d), respectively) it could be concluded that the regeneration was not completely finished by the time the decrease of pressure test started. The steep drop in the amounts of all substances with pressure could be explained by a high deposition of coke that quickly led to the catalyst's deactivation.

Both the results of these three tests lacked of reproducibility. It was noticed that the carbon that was produced in each set could not be removed by a regeneration at 300 ºC, with the exception of the test with EtOH /10% v/v). This could be reversed by an increase of both the reaction and the regeneration operating temperature.

The methane yield was calculated relating to the OMW's TOC present in the feed as follows:

$$Y_{CH_4}(\%) = \frac{F_{CH_4}}{2F_{TOC}} \times 100 \quad (4.7)$$

There were some doubts related to the chemical analysis of the OMW. The analysis reported a TOC of 750 mg L^{-1}, rather lower considering that the phenol's content is in line with previous experiments by Tosti et al. (2015). As such, the methane yield was also calculated considering the TOC of Tosti et al. (2015) of 8694 mg L^{-1}.

The results are reported in Table 4.8 and plotted in Figure 4.14.

Table 4.8 - Percentage of methane yield obtained for the test with OMW.

	TOC = 8694 mg L^{-1}		TOC = 750 mg L^{-1}	
	1 - 3 - 5 bar	5 - 3 - 1 bar	1 - 3 - 5 bar	5 - 3 - 1 bar
1	42.61	3.69	494.29	42.86
3	11.58	3.69	134.29	42.86
5	5.67	7.76	65.71	90.00

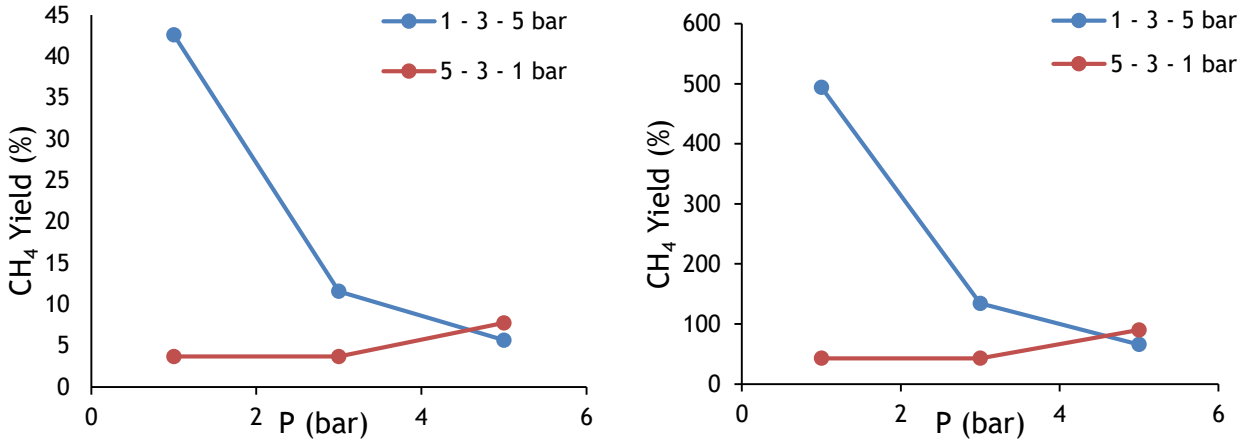

Figure 4.14 - Variation of the methane yield with pressure for the hydrogenolysis of OMW considering a TOC of a) 8694 mg L^{-1} and b) 750 mg L^{-1}.

As can be observed the methane yield considering a TOC of 750 mg L^{-1} is incredibly high, giving cause to doubt the chemical analysis performed by the University of Naples.

If a TOC of 8694 mg L^{-1} is considered, a high methane yield is observed in the beginning of the experiment (at 1 bar, for the "1 – 3 – 5 bar test") which rapidly decreases as the pressure is increased, and the experiment continues, probably due to coke deposition. The regeneration needed more time to be completed seeing that the test "5 – 3 – 1 bar" obtained very low values of methane yield. Also, in order to be more effective, as referred in the previous section, both the regeneration and the reaction itself should have been performed at a higher temperature which will be the goal of a future work at ENEA.

5. Conclusions and Suggestions for Future Work

The research of hydrogen production techniques in an important component for the development of a hydrogen economy. Also, methane is an energy fuel that could easily be inserted in an hydrogen economy due to its easiness in being fed to the already existing infrastructure.

In the case of the hydrogen production via steam reforming reactions, a 10.67 sccm production of hydrogen was achieved at 1 bar, with a feed of 15 g h^{-1} of a previous work's olive mill wastewater (OMW) and 15 sccm of CH_4. This amount was fairly low when compared with said previous work's results which accounted a 34.5 sccm production of hydrogen, with the same feed, at 5 bar. This low hydrogen production results via steam reforming reaction leads to the conclusion that this catalyst is not adequate.

In the case of hydrogen production via oxidative steam reforming, the catalyst behaved even worst, by not being able to produce any amount of hydrogen. At this point, the production of hydrogen course of this work was discontinued and followed to the production of methane via hydrogenolysis reaction.

The highest methane yield observed was of 63.31%, which corresponded to a production of 15.39 sccm, for a feed of ethanol (10% v/v) of 15 g h^{-1} and 110 sccm of hydrogen, matched a H_2/EtOH ratio of 9, at 3 bar. However, the results obtained have different behaviours, possibly due to the high degree of carbon deposition, which led them to lack reproducibility. On all of these tests a high amount of hydrogen was required to produce methane at higher yields, although most of it did not react.

Some doubts about the chemical analysis were raised, and considering a TOC value of 8694 mg L^{-1}, the production of methane from OMW had a maximum of 3.46 sccm (a yield of 42.6%) at 1 bar with a feed of 15 g h^{-1} of OMW and 149 sccm of hydrogen.

As a main conclusion, and reference for future work, it is worth mentioning that although the catalyst used is not adequate for the production of hydrogen, it might be worth to further study the hydrogenolysis reaction for production of methane. It was noted that 300 ºC is not a favourable operating temperature for this reaction, reason why it would be interesting to study the results at a higher temperature.

6. References

Aleklett, Kjell, Mikael Höök, Kristofer Jakobsson, Michael Lardelli, Simon Snowden, and Bengt Söderbergh. 2010. "The Peak of the Oil Age – Analyzing the world oil production Reference Scenario in World Energy Outlook 2008." *Energy Policy* no. 38 (3):1398-1414.

APHA, Andrew D. Eaton, Association American Water Works, and Federation Water Environment. 2005. *Standard methods for the examination of water and wastewater*. Washington, D.C.: APHA-AWWA-WEF.

Crabtree, G. W., M. S. Dresselhaus, and M. V. Buchanan. 2004. "The hydrogen economy." *Physics Today* no. 57 (12):39-44.

de Lima, S. M., I. O. da Cruz, G. Jacobs, B. H. Davis, L. V. Mattos, and F. B. Noronha. 2008. "Steam reforming, partial oxidation, and oxidative steam reforming of ethanol over Pt/CeZrO2 catalyst." *Journal of Catalysis* no. 257 (2):356-368.

Dincer, I., and C. Acar. 2015. "Review and evaluation of hydrogen production methods for better sustainability." *International Journal of Hydrogen Energy*.

Dunn, S. 2002. "Hydrogen futures: Toward a sustainable energy system." *International Journal of Hydrogen Energy* no. 27 (3):235-264.

Fiorentino, Antonio, Alessandra Gentili, Marina Isidori, Pietro Monaco, Angela Nardelli, Alfredo Parrella, and Fabio Temussi. 2003. "Environmental Effects Caused by Olive Mill Wastewaters: Toxicity Comparison of Low-Molecular-Weight Phenol Components." *Journal of Agricultural and Food Chemistry* no. 51 (4):1005-1009.

Gaetano, Presterà. 2014. "Produzione di Idrogeno Ultrapuro da Reforming di Acque di Vegetazione e Metano Mediante Reattori a Membrana", Dipartimento di Ingegneria Civile, Edile e Ambientale, Università degli Studi di Napoli "Federico II".

Gallucci, Fausto, Angelo Basile, and Faisal Ibney Hai. 2011. "Introduction – A Review of Membrane Reactors." In *Membranes for Membrane Reactors*, 1-61. John Wiley & Sons, Ltd.

IEA. 2014. World Energy Outlook 2014. Em *Executive Summary*, editado por Internation Energy Agency. OECD/IEA.

International Olive Oil Council. 2014. Statistics on EU Olive Oil production. http://www.internationaloliveoil.org/estaticos/view/131-world-olive-oil-figures.

Jørgensen, C., and S. Ropenus. 2008. "Production price of hydrogen from grid connected electrolysis in a power market with high wind penetration." *International Journal of Hydrogen Energy* no. 33 (20):5335-5344.

Koros, W. J., Y. H. Ma, and T. Shimidzu. 1996. "Terminology for membranes and membrane processes (IUPAC Recommendations 1996)." *Pure Appl. Chem.* no. 68 (7):1479-1489.

Li, H., H. Xu, and W. Li. 2008. "Study of n value and α/β palladium hydride phase transition within the ultra-thin palladium composite membrane." *Journal of Membrane Science* no. 324 (1-2):44-49.

Morreale, Bryan D. 2002. Evaluation Of Inorganic, Hydrogen Membranes At Elevated Pressures And Temperatures. Master's Thesis. http://d-scholarship.pitt.edu/6292/.

Morris, Craig, and Martin Pehnt. 2014. *Energy Transition: The German Energiewende*. ed Heinrich Böll Foundation. www.energytransition.de.

NOW - National Organization Hydrogen and Fuel Cell Technology. 2014. *Annual Report*. http://www.now-

gmbh.de/fileadmin/user_upload/RE_Publikationen_NEU_2013/Publikationen_NOW_Berichte/NOW_Annual_Report_2014.pdf.

Ockwig, N. W., and T. M. Nenoff. 2007. "Membranes for hydrogen separation." *Chemical Reviews* no. 107 (10):4078-4110.

Palma, Vincenzo, Filomena Castaldo, Paolo Ciambelli, and Gaetano Iaquaniello. 2012. "Sustainable Hydrogen Production by Catalytic Bio-Ethanol Steam Reforming." In *Greenhouse Gases - Capturing, Utilization and Reduction*, edited by Dr Guoxiang Liu. INTECH Open Access Publisher. http://www.intechopen.com/books/greenhouse-gases-capturing-utilization-and-reduction/sustainable-hydrogen-production-by-catalytic-bio-ethanol-steam-reforming.

Pérez, P., C. A. Cornaglia, A. Mendes, L. M. Madeira, and S. Tosti. 2015. "Surface effects and CO/CO2 influence in the H2 permeation through a Pd-Ag membrane: A comprehensive model." *International Journal of Hydrogen Energy* no. 40 (20):6566-6572.

Roig, A., M. L. Cayuela, and M. A. Sánchez-Monedero. 2006. "An overview on olive mill wastes and their valorisation methods." *Waste Management* no. 26 (9):960-969.

Sarić, M., J.W. Dijkstra, S. Walspurger, and W.G. Haije. 2014. "Potential of "Power to Gas" conversion chain integration with Biomethane Production." *ECN*.

Tosti, S., C. Accetta, M. Fabbricino, M. Sansovini, and L. Pontoni. 2013. "Reforming of olive mill wastewater through a Pd-membrane reactor." *International Journal of Hydrogen Energy* no. 38 (25):10252-10259.

Tosti, S., C. Cavezza, M. Fabbricino, L. Pontoni, V. Palma, and C. Ruocco. 2015. "Production of hydrogen in a Pd-membrane reactor via catalytic reforming of olive mill wastewater." *Chemical Engineering Journal* no. 275:366-373.

Tosti, Silvano. 2010. "Overview of Pd-based membranes for producing pure hydrogen and state of art at ENEA laboratories." *International Journal of Hydrogen Energy* no. 35 (22):12650-12659.

Tsagaraki, Evagelia, HarrisN Lazarides, and KonstantinosB Petrotos. 2007. "Olive Mill Wastewater Treatment." In *Utilization of By-Products and Treatment of Waste in the Food Industry*, edited by Vasso Oreopoulou and Winfried Russ, 133-157. Springer US.

Vadrucci, M., F. Borgognoni, A. Moriani, A. Santucci, and S. Tosti. 2013. "Hydrogen permeation through Pd-Ag membranes: Surface effects and Sieverts' law." *International Journal of Hydrogen Energy* no. 38 (10):4144-4152.

Vaidya, P. D., and A. E. Rodrigues. 2006. "Insight into steam reforming of ethanol to produce hydrogen for fuel cells." *Chemical Engineering Journal* no. 117 (1):39-49.

Appendix 1. Calculation of the oxygen flow

The reaction of the oxidative steam reforming of ethanol is the following:

$$C_2H_5OH + 2H_2O + 0.5O_2 \rightarrow 2CO_2 + 5H_2 \qquad \Delta H = -50\ kJ.mol^{-1} \tag{2.21}$$

Equation 2.21 has a C/O_2 ratio of 4:1. According to Tosti et al. (2015) the TOC content of the OMW (the same used in this work) was:

$$[TOC] = 8694\ \frac{mg_{TOC}}{L_{OMW}} \approx 8.7\ \frac{g_{TOC}}{L_{OMW}}$$

Being the density of the OMW is equal to water then,

$$8.7\frac{g_{TOC}}{L_{OMW}} = 8.7 \times 10^{-3}\frac{g_{TOC}}{g_{OMW}}$$

If a flow of 10 g h^{-1} of OMW is considered,

$$8.7 \times 10^{-3}\frac{g_{TOC}}{g_{OMW}}.10\frac{g_{OMW}}{h} = 8.7 \times 10^{-2}\frac{g_{TOC}}{h}$$

Assuming that one gram of TOC equals one gram of carbon then,

$$[TOC] = 8.7 \times 10^{-2}\frac{g_{TOC}}{h}.\frac{1}{12}\frac{mol}{g_{C(TOC)}} = 0.725 \times 10^{-2}\ \frac{mol_{C(TOC)}}{h} = 0.012 \times 10^{-2}\frac{mol_{C(TOC)}}{min}$$

As a ratio of C/O_2 was set in 4:1, then it is needed a flow of O_2 of

$$0.012 \times 10^{-2}\frac{mol_{C(TOC)}}{min} \times \frac{1}{4}\frac{mol_{O_2}}{mol_{C(TOC)}} = 3.02 \times 10^{-5}\frac{mol_{O_2}}{min} = 67.7\frac{cm^3}{min}$$

For a feed of 15 g.h^{-1} of OMW it is necessary a flow of 101.55 sccm of O_2.

- **Oxygen flow corrected from the present OMW**

The OMW used in this work had a TOC value of 750.38 mg L^{-1}. Considering a flow of 15 g h^{-1} of OMW, the amount of carbon being fed is of 5.21x10^{-5} $mol_{C(TOC)}$ min^{-1}. Seeing that 101.55 sccm of O_2 where fed, then the C/O_2 ratio is approximately 1:2.